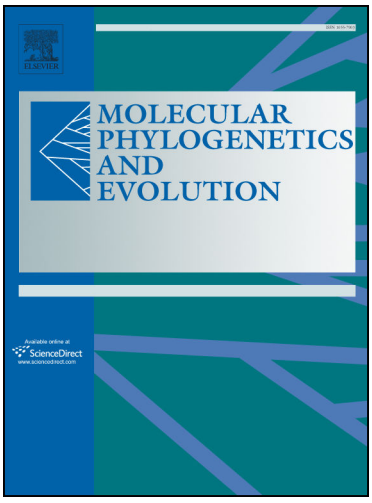

Integrative phylogenetic, phylogeographic and morphological characterisation of the *Unio crassus* species complex reveals cryptic diversity with important conservation implications

M. Lopes-Lima, J. Geist, S. Egg, L. Beran, A. Bikashvili, B. Van Bocxlaer, AE. Bogan, IN. Bolotov, OA. Chelpanovskaya, K. Douda, V. Fernandes, A. Gomes-dos-Santos, DV. Gonçalves, ME. Gürlek, NA. Johnson, I. Karaouzas, Ü. Kebapç ı, AV. Kondakov, R. Kuehn, J. Lajtner, L. Mumladze, K-O. Nagel, E. Neubert, M. Österling, J. Pfeiffer, V. Prié, N. Riccardi, J. Sell, LD. Schneider, S. Shumka, I. Sîrbu, G. Skujienė, CH. Smith, R. Sousa, K. Stöckl, J. Taskinen, A. Teixeira, M. Todorov, T. Trichkova, M. Urbańska, S. Välilä, S. Varandas, J. Veríssimo, IV. Vikhrev, G. Woschitz, K. Zając, T. Zając, D. Zanatta, A. Zieritz, S. Zogaris, E. Froufe

PII: S1055-7903(24)00038-1
DOI: https://doi.org/10.1016/j.ympev.2024.108046
Reference: YMPEV 108046

To appear in: *Molecular Phylogenetics and Evolution*

Received Date: 17 September 2023
Revised Date: 16 February 2024
Accepted Date: 27 February 2024

Please cite this article as: Lopes-Lima, M., Geist, J., Egg, S., Beran, L., Bikashvili, A., Van Bocxlaer, B., Bogan, AE., Bolotov, IN., Chelpanovskaya, OA., Douda, K., Fernandes, V., Gomes-dos-Santos, A., Gonçalves, DV., Gürlek, ME., Johnson, NA., Karaouzas, I., Kebapç ı, Uuml., Kondakov, AV., Kuehn, R., Lajtner, J., Mumladze, L., Nagel, K-O., Neubert, E., Österling, M., Pfeiffer, J., Prié, V., Riccardi, N., Sell, J., Schneider, LD., Shumka, S., Sîrbu, I., Skujienė, G., Smith, CH., Sousa, R., Stöckl, K., Taskinen, J., Teixeira, A., Todorov, M., Trichkova, T., Urbańska, M., Välilä, S., Varandas, S., Veríssimo, J., Vikhrev, IV., Woschitz, G., Zając, K., Zając, T., Zanatta, D., Zieritz, A., Zogaris, S., Froufe, E., Integrative phylogenetic, phylogeographic and morphological characterisation of the *Unio crassus* species complex reveals cryptic diversity with important conservation implications, *Molecular Phylogenetics and Evolution* (2024), doi: https://doi.org/10.1016/j.ympev.2024.108046

Integrative phylogenetic, phylogeographic and morphological characterisation of the *Unio crassus* species complex reveals cryptic diversity with important conservation implications.

Lopes-Lima M[1,2,*]; Geist J[3]; Egg S[3,4]; Beran L[5]; Bikashvili A[6]; Van Bocxlaer B[7]; Bogan AE[8]; Bolotov IN[9]; Chelpanovskaya OA[9]; Douda K[10]; Fernandes V[1,2]; Gomes-dos-Santos A[11]; Gonçalves DV[1,2,11]; Gürlek ME[12]; Johnson NA[13]; Karaouzas I[14]; Kebapçı Ü[15]; Kondakov AV[9]; Kuehn R[4]; Lajtner J[16]; Mumladze L[6]; Nagel K-O[17]; Neubert E[18,19]; Österling M[20]; Pfeiffer J[21]; Prié V[1,2,22]; Riccardi N[23]; Sell J[24]; Schneider LD[25]; Shumka S[26]; Sîrbu I[27]; Skujienė G[28]; Smith CH[29]; Sousa R[30]; Stöckl K[31]; Taskinen J[32]; Teixeira A[33]; Todorov M[34]; Trichkova T[34]; Urbańska M[35]; Välilä S[32]; Varandas S[1,36]; Veríssimo J[1,2]; Vikhrev IV[9]; Woschitz G[37]; Zając K[38]; Zając T[38]; Zanatta D[39]; Zieritz A[40]; Zogaris S[14]; Froufe E[11]

[1]CIBIO, Centro de Investigação em Biodiversidade e Recursos Genéticos, InBIO Laboratório Associado, Campus de Vairão, Universidade do Porto, 4485-661 Vairão, Portugal

[2]BIOPOLIS Program in Genomics, Biodiversity and Land Planning, CIBIO, Campus de Vairão, 4485-661 Vairão, Portugal

[3]Aquatic Systems Biology, Technical University of Munich, TUM School of Life Sciences, Mühlenweg 22, 85354 Freising, Germany

[4]Molecular Zoology, Technical University of Munich, TUM School of Life Sciences, Hans-Carl-von-Carlowitz-Platz 2, Freising, Germany

[5]Regional Office Kokořínsko – Máchův kraj Protected Landscape Area Administration, Nature Conservation Agency of the Czech Republic, Česká 149, CZ-27601 Mělnik, Czech Republic

[6]Institute of Zoology, Ilia State University, Cholokashvili ave. 3/5, 0162, Tbilisi, Georgia

[7]CNRS, Univ. Lille, UMR 8198 – Evo-Eco-Paleo, F-59000 Lille, France

[8]North Carolina Museum of Natural Sciences, 11 West Jones Street, Raleigh, NC 27601 USA

[9]N. Laverov Federal Center for Integrated Arctic Research of the Ural Branch of the Russian Academy of Sciences, Nikolsky Av. 20, 163020 Arkhangelsk, Russia

[10]Department of Zoology and Fisheries, FAFNR, Czech University of Life Sciences Prague, Kamýcká 129, CZ-16500, Prague, Czech Republic

[11]CIIMAR/CIMAR - Interdisciplinary Centre of Marine and Environmental Research, University of Porto, Terminal de Cruzeiros do Porto de Leixões, Av. General Norton de Matos s/n, 4450-208 Matosinhos, Portugal

[12]Burdur Vocational School of Food Agriculture and Livestock, Mehmet Akif Ersoy University, 15100 Burdur, Türkiye

[13]U.S. Geological Survey, Wetland and Aquatic Research Center, Gainesville, Florida, USA.

[14]Hellenic Centre for Marine Research, Institute of Marine Biological Resources and Inland Waters, 46.7 km Athens-Sounio Av., Anavyssos, 19013, Greece.

[15]Biology Department, Faculty of Science and Arts, Burdur Mehmet Akif Ersoy University, Burdur, Türkiye

[16]Department of Biology, Faculty of Science, University of Zagreb, Horvatovac 102a, 10000 Zagreb, Croatia

[17]Malacological Section, Senckenberg Research Institute and Natural History Museum Frankfurt/M., Senckenberganlage 25, 60325 Frankfurt am Main, Germany.

[18]Natural History Museum, 3005 Bern, Switzerland

[19]Institute of Ecology and Evolution, University of Bern, 3012 Bern, Switzerland

[20]Institution of Environmental and Life Sciences, Karlstad University, Biology, 65188 Karlstad, Sweden

[21]National Museum of Natural History, Smithsonian Institution, 10th and Constitution Avenue, Washington, DC, USA

[22]Institut Systématique Evolution Biodiversité (ISYEB), Muséum national d'Histoire naturelle, CNRS, Sorbonne Université, EPHE, Université des Antilles. 57 rue Cuvier, CP 51, 75005 Paris, France

[23]CNR Water Research Institute, Largo Tonolli 50, 28922 Verbania, Italy

[24]Department of Genetics and Biosystematics, Faculty of Biology, University of Gdańsk, Wita Stwosza 59, 80-308 Gdańsk, Poland

[25]The Rural Economy and Agricultural Society, 305 96 Eldsberga, Sweden

[26]Faculty Of Biotechnology and Food, Agricultural University of Tirana, Koder Kamez, Tirana

2029, Albania

[27]Lucian Blaga University of Sibiu, Faculty of Sciences, 5-7 Dr. I. Rațiu St., 550012 Sibiu, Romania

[28]Department of Zoology, Institute of Biosciences, Life Sciences Center, Vilnius University, Saulėtekio av. 7, LT-10223 Vilnius, Lithuania

[29]Department of Integrative Biology, University of Texas, Austin, Texas, USA

[30]CBMA - Centre of Molecular and Environmental Biology, Department of Biology, University of Minho, Campus Gualtar, 4710-057 Braga, Portugal

[31]Bavarian Academy for Nature Conservation and Landscape Management, Seethalerstrasse 6,

83410 Laufen, Germany

[32]Department of Biological and Environmental Science, University of Jyväskylä, P.O. Box 35, 40014 University of Jyväskylä, Finland

[33]Centro de Investigação de Montanha (CIMO), Instituto Politécnico de Bragança, Campus de Santa Apolónia, 5300-253 Bragança, Portugal

[34]Institute of Biodiversity and Ecosystem Research, Bulgarian Academy of Sciences, 1 Tsar Osvoboditel Blvd., 1000 Sofia, Bulgaria

[35]Department of Zoology, Poznań University of Life Sciences, ul. Wojska Polskiego 28, 60-637

Poznań, Poland

[36]CITAB-UTAD - Centre for Research and Technology of Agro-Environment and Biological Sciences, University of Trás-os-Montes and Alto Douro, Forestry Department, Vila Real, Portugal.

[37]IFIS - Ichthyological Research Initiative Styria, 1160 Vienna

[38]Institute of Nature Conservation, Polish Academy of Sciences, Al. Adama Mickiewicza 33, 31-120 Kraków, Poland

[39]Biology Department, Institute for Great Lakes Research, Central Michigan University, Mount Pleasant Michigan 48859, USA.

[40]School of Geography, University of Nottingham, University Park, Sir Clive Granger Building, Nottingham NG7 2RD, United Kingdom.

AUTHOR CONTRIBUTIONS:

Study conception and design MLL, JG, SE, EF

Draft manuscript preparation: MLL with text contributions by BVB, JG, AZ

Laboratory work (genetics): SE, BA, OAC, AGS, VF, AVK, RK

Molecular Analyses: MLL, BVB, NJ, AGS, JP, CHS, JV, EF

Fossil calibration: BVB

Morphometry: AZ

Taxonomy: MLL, AEB, K-ON, VP

Fieldwork: MLL, SE, JG, LB, AEB, AB, INB, OAC, KD, DVG, MEG, IK, AVK, JL, UK, RK, MÖ, VP, NR, LDS, IS, SG, SR, SS, JS, KS, JT, AT, MT, TT, LM, MU, SVäl, SVar, IVV, KZ, TZ, SZ

All authors contributed to the interpretation of the results and the final version of the manuscript.

ABSTRACT

The global decline of freshwater mussels and their crucial ecological services highlight the need to understand their phylogeny, phylogeography and patterns of genetic diversity to guide conservation efforts. Such knowledge is urgently needed for *Unio crassus*, a highly imperilled species originally widespread throughout Europe and southwest Asia. Recent studies have resurrected several species from synonymy based on mitochondrial data, revealing *U. crassus* to be a complex of cryptic species. To address long-standing taxonomic uncertainties hindering effective conservation, we integrate morphometric, phylogenetic, and phylogeographic analyses to examine species diversity within the *U. crassus* complex across its entire range. Phylogenetic analyses were performed using cytochrome c oxidase subunit I (815 specimens from 182 populations) and, for selected specimens, whole mitogenome sequences and Anchored Hybrid Enrichment (AHE) data on ~600 nuclear loci. Mito-nuclear discordance was detected, consistent with mitochondrial DNA gene flow between some species during the Pliocene and Pleistocene. Fossil-calibrated phylogenies based on AHE data support a Mediterranean origin for the *U. crassus* complex in the Early Miocene. The results of our integrative approach support 12 species in the group: the previously recognised *Unio bruguierianus*, *Unio carneus, Unio crassus*, *Unio damascensis*, *Unio ionicus*, *Unio sesirmensis*, and *Unio tumidiformis*, and the reinstatement of five nominal taxa: *Unio desectus* **stat. rev.**, *Unio gontierii* **stat. rev.**, *Unio mardinensis* **stat. rev.**, *Unio nanus* **stat. rev.**, and *Unio vicarius* **stat. rev.** Morphometric analyses of shell contours reveal important morphospace overlaps among these species, highlighting cryptic, but geographically structured, diversity. The distribution, taxonomy, phylogeography, and conservation of each species are succinctly described.

Keywords: conservation; freshwater mussels; phylogeography; Unionida

1. Introduction

Various groups of animals display visual resemblances until they are subjected to comprehensive analyses, including both morphological and molecular characterisation. In species that have been extensively studied over time, cryptic diversity refers to two or more taxa that are so closely morphologically similar that they can only be distinguished by molecular examination or by considering their allopatric distributions (Struck et al., 2018). Such similarity hinders reliable species delimitation and prevents accurate estimates of species-level diversity. These limitations may complicate taxon-based management, especially in animal groups of conservation concern, such as freshwater bivalves of the order Unionida, or freshwater mussels. These animals are receiving scientific and societal attention due to their high ecological importance and

imperilled status (Lopes-Lima et al., 2014, 2018; Walker et al., 2014; Ferreira-Rodríguez et al., 2019; Sun et al., 2019; Aldridge et al., 2023a). Some mussel species simultaneously fulfil the criteria of indicator, umbrella, and flagship species, making them an important group of species for prioritising conservation and restoration actions for aquatic ecosystems (Geist, 2010, 2011; Lopes-Lima et al., 2020).

Unio Philipsson in Retzius, 1788, is the type genus of the most species-rich freshwater mussel family, Unionidae and of the order Unionida. It is predominantly a western Palaearctic genus with a core distribution in Europe but extending to western and central Asia and northwestern Africa, with disjunct distributions in other African regions, namely the Somali Peninsula and South Africa (Araujo et al., 2018; Lopes-Lima et al., 2017a). *Unio* populations occupy a variety of different freshwater habitats, ranging from streams and rivers to lakes and wetlands (Lopes-Lima et al., 2017b). Species boundaries within the genus *Unio* are notoriously difficult to establish due to the high degree of intraspecific plasticity in shell morphology and the scarcity of diagnosable shell morphological characters across species (Zieritz et al., 2010; Prié and Puillandre, 2014; Klishko et al., 2017). For these reasons, *Unio* has many nominal taxa (more than 1,100), and its taxonomy and systematics were unstable until the mid-20th century (Graf, 2010). The taxonomy of *Unio* only began to stabilise in the late 1960s with the publication of a comprehensive morphology-based revision of the species diversity and taxonomy of freshwater mussels worldwide (Haas, 1969).

The introduction of molecular sequencing at the end of the 20th century helped to gain understanding into the evolutionary relationships of *Unio* in some regions of Europe and Asia (e.g. Araujo et al., 2005, 2009, 2018; Reis and Araujo, 2009; Prié et al., 2012; Froufe et al., 2016), but the available molecular data remain mostly limited to mitochondrial DNA (mtDNA) markers (but see e.g. Froufe et al., 2016 or Feind et al., 2018). Although mitochondrial and nuclear sequencing data are generally concordant at the species level in freshwater mussels (e.g. Pfeiffer et al., 2019; Smith et al., 2020; Neemuchwala et al., 2023), there have been a few reported cases of incongruence between these markers in certain genera due to hybridisation and introgression (Chong et al., 2016; Sano et al., 2022).

Unio is currently divided into four distinct mitochondrial clades (Lopes-Lima et al., 2017b; Araujo et al., 2018). The *gibbus* clade contains only two species found in northwestern Africa, one of which also occurs in the southern tip of the Iberian Peninsula (Araujo et al., 2009; Khalloufi et al., 2011). The *tumidus* clade is currently represented by a single species, *Unio tumidus*, which is widespread across northern Europe and the edges of western Asia (Lopes-Lima et al., 2017b; Babushkin et al., 2021). The *pictorum* and *crassus* clades are each represented by several closely related species across the Western Palearctic (Froufe et al., 2016, 2017; Araujo et al., 2018; Lopes-Lima et al., 2021). The phylogeography of these clades appears to reflect ancient patterns of vicariance (Nagel, 2000) driven by the complex geological and climatic history of the European continent over the past few million years (Hewit et al., 1999; Goméz and Lunt, 2007; Lang et al., 2011).

Due to its conservation importance (see below), the *crassus* clade (here referred to as the *U. crassus* complex) has been the most studied *Unio* clade in recent years (Lopes-Lima et al., 2017b). Haas (1969) considered *U. crassus* as a single species but divided it into eight subspecies, which have since been studied to varying degrees (Fig. 1). Recent studies investigating the evolutionary history of the group have led to the elevation of four subspecies (*U. c. bruguierianus*, *U. c. carneus*, *U. c. ionicus*, and *U. c. mongolicus*) to the species level (Araujo et al., 2018; Klishko et al., 2019; Bolotov et al., 2020; Lyubas et al., 2022). However, *U. c. mongolicus* was reassigned to a different genus, namely *Middendorffinaia* (Klishko et al., 2019). The other four subspecies considered by Haas (1969) remain as synonyms of *U. crassus* (Graf and Cummings, 2023; Molluscabase, 2023). In addition to the subspecies of Haas (1969), three other nominal taxa have been resurrected from synonymy based on recent morphological and molecular work, namely the Iberian *U. tumidiformis* (Reis and Araujo, 2009) and the eastern Mediterranean *U. damascensis*

and *U. sesirmensis* (Lopes-Lima et al., 2021). The current taxonomic consensus (Graf and Cummings, 2023; Molluscabase, 2023) recognizes the *U. crassus* complex as consisting of seven species: *U. crassus* in the northern regions of Europe, from France to Russia, and six other species, each restricted to either Iberia, the Balkans, Anatolia or the Levant. Other divergent mtDNA lineages have been detected within the *U. crassus* complex, including two in Greece (Araujo et al., 2018) and two in France and Poland (Prié and Puillandre, 2014; Kilikowska et al., 2020), but their taxonomic status has not been assessed due to the conflicting evidence from morphological and mtDNA datasets and the lack of comprehensive geographic sampling.

As with many unionoids, previous systematic and phylogenetic studies of the *U. crassus* complex have relied primarily on mtDNA and morphological data. No study to date has used nuclear DNA to reconstruct the evolutionary history of *Unio* or to test previous species' hypotheses based on mitochondrial data. A recently developed freshwater mussel-specific target capture approach (Pfeiffer et al., 2019) has been successfully used to reconstruct both deep and shallow relationships using >500 nuclear gene fragments (Pfeiffer et al., 2019, 2021; Smith et al., 2020; Gomes-dos-Santos et al., 2023; Neemuchwala et al., 2023). In addition, whole mitochondrial genomes are becoming increasingly available, and the use of whole mitochondrial gene sets for phylogenetic inference allows for a more thorough estimation of mitochondrial evolution (e.g., Froufe et al., 2020). Contrasting and/or combining information from nuclear and mitochondrial genes may provide a more comprehensive understanding of the evolutionary relationships within *Unio* and reveal potential mito-nuclear discordance, as reported for other freshwater taxa (e.g. Waters et al., 2010; Campbell et al., 2022).

Due to the taxonomic history outlined above, *U. crassus* was considered to be a single species in 1992 when the main legal policy for the conservation of species and habitats in the European Union, the Habitats Directive, was implemented. Under this policy, *U. crassus* was listed as one of the few invertebrate species of conservation concern, requiring EU countries to protect, monitor, and designate special areas for its conservation. As a result, *U. crassus* is a target species of the EU's 'Life' conservation programme, which has so far contributed around €20 million to the conservation of this species and its habitats across Europe (Mammola et al., 2020; EC, 2023). Given the high level of conservation concern, it is crucial to accurately understand the patterns of genetic diversity in the *U. crassus* complex to better inform conservation efforts and management, which is particularly relevant in the context of the increasing number of captive breeding efforts for *U. crassus* across Europe (Geist et al., in press).

Using a *cytochrome c oxidase subunit I* (COI) of 815 *U. crassus* individuals from 182 sampling locations (hereafter populations) across its distribution, coupled with whole mitogenomes and approximately 600 nuclear gene fragments from individuals of selected populations, we aim to: **i**) establish a phylogenetic framework of the *U. crassus* complex using nuclear markers; **ii**) compare phylogenies constructed with nuclear and mitochondrial data to evaluate mito-nuclear concordance; **iii**) clarify the taxonomic status and biogeography of species within the *U. crassus* complex; **iv**) characterise the geographic distribution of genetic variation; and **v**) provide updated conservation management guidance for all delineated species.

2. Materials and methods

2.1. Taxon sampling

Tissue or haemolymph samples from a total of 509 specimens belonging to the *U. crassus* complex were collected from 105 populations in 23 different countries for DNA extraction, sequencing, and subsequent molecular analyses (Fig. 1; Table S1). Available samples from 8

additional taxa representing other genera within the Unioninae were also selected for extraction and included as the outgroup in subsequent COI, whole mitogenome, and AHE phylogenies (Tables S1-S3). These outgroup taxa were specifically selected to facilitate fossil-based time-calibration of the diversification history of the *U. crassus* complex. Of the 509 genetically analysed specimens, 399 were photographed for morphometry in the field before being returned to their habitats. Additional images of 147 specimens for which COI sequences were previously published by the co-authors were also included in the morphometric analyses (see below). Field sampling has been conducted in line with national and international regulations, with the appropriate permits.

2.2. DNA extraction, amplification, and sequencing

A small sample of foot tissue or haemolymph was collected from each specimen following the non-lethal procedures of Naimo et al. (1998) and Geist and Kuehn (2005). Genomic DNA was extracted using a standard high-salt protocol (Sambrook et al., 1989). For each sampled population, 1 to 10 (mean = 4.8) specimens were sequenced for female (F-type) COI. PCR conditions (using the primer set LCO22me2 + HCO700dy2; Walker et al., 2006, 2007) were described in Froufe et al. (2016) with an annealing temperature of 50 °C. Amplified DNA templates were purified and sequenced bidirectionally using the same primers.

A complete F-type mitogenome was sequenced for each major lineage of the *U. crassus* complex, except for those for which a mitogenome sequence was already available (Table S2). Sequencing and assembly of the mitogenome followed Teiga-Teixeira et al. (2020) whereas annotation was completed following Gomes-dos-Santos et al. (2023).

2.3. COI phylogenetic analyses, and species delineation

A COI dataset was aligned using MAFFT v. 7.304 (Katoh and Standley, 2013) with the novel (n = 509) and all previously available sequences (n = 306) belonging to the *U. crassus* complex (Table S1). The COI dataset was then reduced to unique haplotypes (hereafter reduced COI dataset; see Table S1 for haplotype codes) and analysed using Maximum Likelihood (ML) and Bayesian Inference (BI) methods in IQ-TREE v 2.2.0 (Minh et al., 2020) and MrBayes 3.2.7a (Ronquist et al., 2012), respectively. Sequences from *U. pictorum* and *U. delphinus* were selected as the outgroup based on Lopes-Lima et al. (2017b) (Table S1). For the BI analyses, the best-fit models of nucleotide substitution and partition schemes were selected using PartitionFinder 2 (Lanfear et al., 2016) under the Bayesian Information Criterion. The BI analyses were started with program-generated trees and four Markov chains with default incremental heating. Two independent runs of 20×10^6 generations were sampled at 1,000 generation intervals, resulting in a total of 20,000 trees. Burn-in (25%) was determined by convergence of log-likelihood and parameter values using Tracer 1.7.1 (Rambaut et al., 2018). For ML phylogenetic analyses, best-fit models of nucleotide substitution and partitioning schemes were selected using ModelFinder (Kalyaanamoorthy et al., 2017). Maximum likelihood analyses were then performed with an initial tree search, followed by 10 independent runs and 10,000 ultrafast bootstrap replicates.

Four different methods were applied to the total COI dataset to determine the number of molecular operational taxonomic units (MOTUs). The Barcode Index Number (BIN) system was applied using the Cluster Sequences tool as implemented in BOLD 4 (http://v4.boldsystems.org) (Ratnasingham and Hebert, 2013). Assemble Species by Automatic Partitioning (ASAP) was applied using its online version (https://bioinfo.mnhn.fr/abi/public/asap/) with the default settings and the Kimura 2-parameter (K2P) distance matrix (Puillandre et al., 2021). The third method used haplotype network reconstructions in TCS 1.21 (Clement et al., 2000) with a statistical

parsimony limit of 95%. Finally, the fourth method used the Bayesian implementation of the Poisson Tree Processes model (bPTP) (Zhang, Kapli, Pavlidis, & Stamatakis, 2013). To do this, a BI phylogenetic tree of the total COI dataset was constructed using the same parameters as the BI analysis of the reduced COI dataset above. The resulting tree was then used as input to the bPTP web server (available at: http://species.h-its.org/) with 1×10^6 iterations of MCMC and 20% burn-in. Sequence divergence (uncorrected *p*-distance) was estimated using MEGA X (Kumar et al., 2018) to examine genetic differentiation between lineages. For the mitogenome and AHE datasets, species delineation was not performed due to insufficient coverage of intraspecific variability, i.e. only one or very few individuals per species were included in these datasets (see sections 2.4 and 2.5 below).

A Principal Coordinates Analysis (PCoA) was performed on the ingroup of the reduced COI dataset, using the ade4 R-Package (Dray and Dufour, 2007). The first three coordinates were transformed into a colour palette using the RGB algorithm of the adegenet R-Package (Jombart, 2008) to visualise similarities or dissimilarities in the data. Specimens with the same genetic constitution are represented by the same colour. The PCoA was then repeated on the same dataset but excluding all the sequences from the most divergent species (i.e., *U. tumidiformis*) to obtain more resolution of the differences between the remaining species.

2.4. Whole mitogenome phylogenies

A total of 8 specimens spanning the different COI and AHE clades (see COI and AHE results) of the *Unio crassus* complex were selected for the whole mitogenome dataset, complemented by four other mitogenomes already publicly available (Table S2). Ten additional mitogenomes, including 5 *Unio* species (outside the *U. crassus* complex) and 5 more divergent unionids, were selected based on their utility for fossil-based time calibration (Table S2). The sequences of all mtDNA protein-coding genes (PCG), excluding the sex-specific open reading frames (H-ORF and F-ORF; Breton et al., 2011), were used in the phylogenetic analyses. Sequences of each gene were aligned using MAFFT and trimmed using GUIDANCE2 (Sela et al., 2015; see Froufe et al., 2016 for parameters used). Gene alignments were then concatenated, resulting in a dataset with a total of 13,449 aligned nucleotide positions. Phylogenies were estimated using ML and BI methods following the same procedures as described above.

2.5. Sample selection and AHE sequencing and data processing

A total of 31 samples covering all mitochondrial lineages were selected for the AHE dataset (Table S3), covering distinct river basins and/or distinct morphotypes. In addition, one specimen of *U. tumidus*, *U. delphinus*, *U. terminalis*, and *U. pictorum* were selected for AHE sequencing outgroups along with six other species (*Lanceolaria lanceolata*, *Anodonta anatina*, *Anodonta cygnea*, *Nodularia douglasiae*, *Cuneopsis pisciculus*, and *Unio gibbus*) with publicly available AHE data (Pfeiffer et al., 2019; Table S3). DNA extraction for each sample was performed as described above, and genomic libraries were enriched using target capture with the Unioverse bait set (Pfeiffer et al., 2019). Genomic DNA was sent to RAPiD Genomics (Gainesville, FL, USA) for library preparation, target enrichment and Illumina sequencing. The procedure consisted of shearing genomic DNA into ~400 bp fragments, which were end-repaired, and an adenine residue was ligated to the 3-end of each blunt-end fragment. Ligation with barcode adaptors was then performed and the library was amplified by PCR. Solution-based target enrichment of pooled libraries was performed using the SureSelectxt Target Enrichment System for Illumina Paired-End Multiplexed Sequencing. Probes had been synthesised as custom SureSelect probes from AgilentTechnologies (Santa Clara, CA, USA) and 150 bp paired-end reads were generated on an Illumina HiSeq 3000 sequencer (San Diego, CA, USA).

AHE sequencing results were processed using the pipeline described by Breinholt et al. (2018). Reads were filtered and quality-trimmed using TRIM GALORE! v0.4.4 (www.bioinformatics.babraham.ac.uk/projects/trim_galore/). Individual locus assemblies were then obtained using iterative bait assembly (IBA.py: Breinholt et al., 2018), specifying the Unioverse probe reference sequences as baits (Pfeiffer et al., 2019). MAFFT v 7.453 (Katoh & Standley, 2013) was used to add the newly generated de novo locus assemblies to the Unioverse reference taxon alignment (options '-addlong' and '-adjustdirectionaccurately'). Isolation of probe and flanking regions for each locus was then performed using the script extract_probe_region.py (Breinholt et al., 2018), and gene orthology was validated using the script ortholog_filter.py (Breinholt et al., 2018), selecting single-hit sequences mapping to the same regions of the *Bathymodiolus platifrons* (Bivalvia: Mytilidae) genome assembly and the Unioverse reference sequence. Individual alignments for each locus were obtained using the script split.py (Breinholt et al., 2018), aligned with MAFFT and FASconCAT-G v 1.04 (Kück and Longo, 2014), used to generate a single consensus sequence of each locus isoform. Finally, the script remove_duplicates.py (Breinholt et al., 2018) was used to discard duplicated loci (putative paralogs sequences).

2.6. AHE datasets and phylogenomic analyses

Phylogenetic inferences were constructed for three datasets, one containing only the target regions, one containing only the flanking regions, and the third containing both the target and flanking regions for each locus. Sequences from each locus, as identified by the AHE pipeline described above, were aligned to reference sequences using MAFFT. Loci present in less than 70% of the samples were excluded. Putative problematic sequences were removed using the scripts alignment_DE_trim.py and flank_dropper.py (Breinholt et al., 2018) and after splitting using extract_probe_region.py to generate the abovementioned three alignment files for each locus, i.e. head (flanking region), target region and tail (flanking region). The final datasets were constructed as follows: target region alone; head+tail; and head+target region+tail. Finally, each dataset was re-aligned using MAFFT and triamAL v. 1.2 (Capella-Gutiérrez et al., 2009) to remove positions with gaps in 50% or more of the sequences. Individual alignments were concatenated using FASconCAT-G (Kück and Longo, 2014).

Phylogenomic analyses were performed using ML and BI as described above. The only difference was the use of ModelFinder to select the best partitioning in scheme and substitution models with the option '-rcluster 10'. IQ-TREE analyses were performed on all datasets. We performed BI on only the head+target region+tail dataset in MrBayes. This used the GTR + I + G model and each chain started with a randomly generated tree and ran for 20×10^6 generations with a sampling frequency of 1 tree every 10,000 generations.

2.7. Phylogeny with fossil-calibrated divergence time

Phylogenetic inference was performed in Beast v. 2.7.2 (Bouckaert et al., 2019) using three fossil calibration points to estimate divergence time (see below). These analyses were performed on two datasets, namely an alignment of the entire maternally-inherited mitogenome sequences of 22 unionids (13,418 bp) and the total AHE dataset for 41 taxa, i.e. the retained head + target region + tail dataset (514,762 bp). Analyses were performed with linked site models, linked clock models, and linked trees, using an HKY substitution model with all parameters estimated, a gamma category count of 4 and empirical state frequencies. An optimised relaxed clock and a calibrated Yule tree model were used for the analysis. Two independent runs were performed for each dataset, using 100×10^6 generations in the MCMC, with 10×10^6 pre-burn-in generations and subsequent sampling every 10,000 samples, resulting in 10,000 trees. Tracer

v. 1.7.2 (Rambaut et al., 2018) was used to verify that runs had reached steady-state conditions. A parameter was considered to have reached stationary conditions when its ESS value was >200, and analysis continued until all parameters reached ESS >>200. Maximum clade credibility (MCC) trees were generated using TreeAnnotator v. 2.7.2 after 10% burn-in and with median node heights (Bouckaert et al., 2019). The MCC trees were then visualised using FigTree v.1.4.4 (http://tree.bio.ed.ac.uk/software/figtree).

Fossil calibration was performed with two calibration points relating to deeply divergent outgroup taxa, whereas the third calibration point relates to *Unio*. The first calibration point relates to the most common recent ancestor (MRCA) of *Anodonta* and *Lanceolaria*. *Anodonta* species have large oval to suboval, very thin shells with edentate hinges as synapomorphic characters, whereas *Lanceolaria* has conspicuously elongate, narrow, sword-shaped shells. The earliest *Anodonta* fossils are Campanian in age (Henderson, 1935; Johnston and Hendy, 2005), whereas the earliest unambiguous *Lanceolaria* are middle to upper Late Cretaceous in age (Gu, 1998; roughly coeval with the earliest *Anodonta*). More detailed information on the fossil assignment and dating strategy is provided in Sup. Appendix 1. We used a lognormal prior with a mean of 83.0 Ma and a standard deviation of 8.5 Ma, covering the entire Late Cretaceous.

The second calibration point is the MRCA of *Cuneopsis* and *Nodularia*. Dating the oldest *Unio* was considered, but as many old unionoid fossils have been grouped into *Unio*, dating of the MRCA of *Unio* was deemed too unreliable. More information is provided in Sup. Appendix 1, but the Paleogene Na Duong formation in northern Vietnam contains *Cuneopsis quangi*, which may be the oldest *Cuneopsis* to date, and *Nodularia cunhatia*, although this taxon lacks certain diagnostic characters of *Nodularia* (Schneider et al., 2013; see also Chen, 1987). A lognormal prior with a mean of 37.0 Ma and a standard deviation of 8.5 Ma was used, which would assign reasonable probabilities to the divergence of *Cuneopsis* and *Nodularia* in the Paleocene, Eocene, or Oligocene.

As a third calibration point, we dated the MRCA of *U. pictorum* and *U. delphinus*, which are difficult to distinguish based on shell morphology but occur in separate geographical regions. Therefore, fossils that can be assigned to *U. pictorum* from within its current geographic range, were used. Within this range, *U. pictorum* can be distinguished from *U. tumidus* and *U. crassus* based on its more elongate, elliptical shape. The oldest fossils that are attributed to *U. pictorum* are from southwestern Siberia and the Middle Pliocene in age (Zykin, 1979, 2012; Klishko et al., 2017; see Sup. Appendix 1). Therefore, a lognormal prior was used for the MRCA of *U. pictorum*/*delphinus* with a mean age of 5.5 Ma and a standard deviation of 1.5 Ma.

As analyses in Beast are concerned with the joint reconstruction of topology and divergence time estimation, we verified our dating strategy using pyr8s (Sanderson, 2003), which allows dating a provided phylogeny. We used the BI and ML phylogenies for the mitogenome and AHE datasets in combination with the age ranges of 61-110 Ma, 23-57 Ma and 3-9 Ma for the three abovementioned calibration points, respectively. Dating with pyr8s was performed under penalized likelihood.

2.8. Morphometric analyses

Based on the phylogenetic analyses and species delineation results, 12 operational taxonomic units were identified as valid species using multiple nuclear and mitochondrial markers (see discussion below and Table 1).

We conducted Fourier Shape Analyses following Crampton and Haines (1996) to assess differences in sagittal shell outline among these operational taxonomic units. In total, 546 specimens from 135 populations (i.e. species-sites) were included in this analysis: *U.*

bruguierianus (67 specimens from 14 sites), *U. carneus* (16 from 4), *U. crassus* s. str. (156 from 40), *U. nanus* (163 from 46), *U. damascensis* (24 from 7), *U. desectus* (11 from 2), *U. gontierii* (12 from 1), *U. ionicus* (12 from 2), *U. mardinensis* (15 from 2), *U. sesirmensis* (10 from 4), *U. tumidiformis* (5 from 1), and *U. vicarius* (55 from 12) (see Table S1 for details).

The outer left valve of each specimen was photographed in vertical projection to obtain an undistorted image of the sagittal outline and a consistent contrast between the shell outline and the background (including minimisation of shadows). Shell outlines of specimens were digitised into xy-coordinates using the program IMAGEJ (Rasband, 2008). The digitised outlines were then subjected to Fast Fourier transformation using the program HANGLE, applying a smoothing normalisation of 20 to eliminate high-frequency pixel noise (Crampton and Haines, 1996). Discarding the first harmonic, which did not contain any shape information, resulted in a set of 18 Fourier coefficients per individual. After rotating outlines to maximum overlap with the program HTREE, a Principal Component Analysis (PCA) was performed on the 18 Fourier coefficients using the program PAST4 (Hammer and Harper, 2013). Synthetic outlines of extreme shell forms were drawn using the program HCURVE as described by Crampton and Haines (1996).

To test for statistical differences in overall sagittal shell shape between species, we conducted Analyses of Variance (ANOVAs) on the first two PC-axes and carried out an Analysis of Similarities (ANOSIM; 9,999 permutations, Euclidean distance) and Discriminant Analysis (DA) on the set of 18 Fourier coefficients. Statistical analyses were conducted in PAST4 (Hammer and Harper, 2013) (PCAs, DAs, ANOSIM), and R version 3.6.3 (ANOVAs and Tukey's *posthoc* pairwise comparisons).

2.9. Taxonomy, systematics, and distribution

A taxonomic re-evaluation of all 12 operational taxonomic units identified here as valid species belonging to the *U. crassus* complex was carried out by comparing biogeographical and morphological characters with the existing type specimens for each nominal taxon (where available) and the available molecular data presented. The type material analysed is listed in Sup. Appendix 2. When types were not found or otherwise unavailable for examination, figured specimens or high-quality photographs were examined. The distribution of each species was inferred using current data and distribution data from Haas (1969), Lopes-Lima et al. (2017b), the MUSSELp (Graf and Cummings, 2023), the IUCN and the GBIF databases (IUCN, 2023; GBIF, 2023). Distribution data were then integrated and presented as coloured potential distribution maps using the level 6 HydroBASINS (Lehner et al., 2013) shapefile, with small sub-basins grouped with their main drainage or with other small drainages (particularly along coastlines). The distribution maps of *U. damascensis* and *U. sesirmensis* have recently been published (Lopes-Lima et al., 2021) and are therefore not shown here. The distributions of the *Unio crassus* subspecies of Haas (1969) were inferred from the overlap of the same hydrographic layers as above and the approximate type locality of all nominal taxa under each subspecies according to the same author and corrected using his distribution comments for each subspecies. For illustrative purposes, vector and raster map data of Earth topography layers from Natural Earth < http://naturalearthdata.com > were also included.

3. RESULTS

3.1. Sequencing outputs and data description

All newly sequenced COI and mitogenome sequences are available on GenBank (see tables S1-S3) and the Mitogenomes and AHE alignments are here included as supplementary material (Supplementary Appendixes 3 and 4).

3.2. COI dataset, phylogenies, species delineation methods, and PCoA.

The COI alignment is 657 bp and contains no indels or stop codons. The dataset was partitioned into the 3 codons, and nucleotide substitution models for the 1st, 2nd and 3rd codon positions were 1) K2P + I, 2) F81, and 3) GTR + I for the BI analysis; and 1) TNe+G4, 2) F81+F, and 3) TPM3+F+I for the ML analysis.

The BI and ML phylogenetic analyses for COI present similar topologies (Figs. 2 and S1). Within the ingroup, the first five splits are clades corresponding to individuals belonging to the southern European species *U. tumidiformis*, *U. sesirmensis*, *U. desectus*, *U. damascensis*, and *U. ionicus*. The remaining clade is not well resolved and contains a polytomy split into three clades, including individuals from the remaining seven species in the *U. crassus* complex (Figs. 2 and S1).

Except for BOLD, which does not separate *U. vicarius* from *U. bruguierianus*, all the species delineation methods give the same result dividing the COI dataset into 10 MOTUs, which we recognise here as valid species (see Discussion) (Figs. 2 and S1). The average COI divergence (uncorrected *p*-distance) between all species is 4.9% ± 2.1 and ranges from 1.1% (between *U. crassus* s. str. and *U. gontierii*) to 9.8% (between *U. tumidiformis* and *U. sesirmensis*) (Table 1).

The PCoA with all species of the *U. crassus* complex shows the existence of five clusters, one highly dissimilar to all others corresponding to *U. tumidiformis* and then four relatively closer clusters representing *U. crassus* s. str., *U. nanus*, *U. ionicus,* and all remaining species from the Balkans and Anatolia, respectively (Fig. S2). The PCoA without sequences from *U. tumidiformis* allows a better resolution and it is possible to see the separation of the mtDNA of *U. crassus* s. str. and *U. nanus*, as well as the populations of western vs. eastern Greece and northern vs. southern Anatolia (Fig. 3).

3.3. Mitogenome structure and assemblies

The newly sequenced mitogenomes contain the typical 13 protein-coding genes (PCGs), 22 transfer RNA and two ribosomal RNA genes (Boore, 1999). Their sizes are within the expected range of F-type mitogenomes for freshwater mussels, and all have the same previously described gene order, i.e. UF1 (Lopes-Lima et al., 2017c). Their main characteristics, including size, gene composition and order can be downloaded from GenBank (Table S2).

3.4. Mitogenome phylogenies

The results of the BI and ML phylogenetic analyses for the mitogenome dataset present similar topologies, so only the BI phylogeny is shown (Fig. 4). Most of the branches are well-supported in the BI phylogeny, except for the position of *U. damascensis*, *U. desectus*, and *U. ionicus* (Fig. 4). Within the ingroup, the first five splits delimit clades of individuals belonging to the same southern European + Anatolian species as in the COI phylogeny (Figs. 2), while the remaining species were arranged into two clades (Fig. 4) rather than three clades as in the COI phylogeny (Fig. 2).

3.5. Anchored Hybrid Enrichment datasets

The total number of IBA assembled sequences per sample varies between 730 (*U. ionicus*) and 1,396 (*N. douglasiae*), with a mean of 872 assembled sequences (Table S3). The mean sequence length of the IBA assemblies per sample ranged from 686.46 bp (*U. carneus*) to 1,423.18 bp (*U. sesirmensis*), with an overall mean sequence length of 1,193.75 bp (Table S3). The number of loci captured after assembly ranges from 598 (*U. ionicus*) to 615 (*A. cygnea*), with an average of 603 (Table S3). Finally, the number of loci retained after the entire Breinholt et al. (2018) AHE processing pipeline ranges between 404 (*A. anatina*) and 608 (*C. pisciculus*), with an average of 488 loci (Table S3).

3.6. Anchored Hybrid Enrichment phylogenies

The BI and ML phylogenetic analyses for the AHE dataset using both the target and the flanking regions yielded the same topologies (Fig. 4). With two exceptions in the ML analyses, all nodes in the phylogenies are well supported (Fig. 4). Within the ingroup, the first three splits represent clades of individuals belonging to five southern European and Anatolian species, the first with the Iberian *U. tumidiformis*, the second with the southwestern Balkan *U. carneus* and *U. ionicus*, and the third with the Anatolian species *U. sesirmensis* and *U. damascensis* (Fig. 4). The remaining clade is divided into two subclades, one containing the south-eastern European and Anatolian species *U. bruguierianus*, *U. gontierii* and *U. mardinensis*, and the other containing the remaining four species with either a wide distribution across Europe (i.e. *U. crassus* s. str. and *U. nanus*) or (predominantly) in the Balkans (*U. desectus* and *U. vicarius*) (Fig. 4). Comparing the AHE phylogenies using the target + flanking regions with those using only the flanking regions, the topology is the same, differing only in the higher support for the AHE probe + flanking for some nodes (Figs. 4 and S3). The topology of the AHE target region phylogenies is similar to the target + flanking and flanking phylogenies in the initial divergence events but unresolved in several of the shallower branches (Figs. 4, S3-S4).

3.7. Time-calibrated phylogenies

The time-calibrated phylogenies as obtained with Beast and pyr8s gave highly similar topologies and divergence times, indicating that our dating strategy was overall robust. In what follows, we report the Beast estimates.

3.7.1 Mitogenomes

The time-calibrated mitogenome phylogeny shows the same topology as the BI and ML mitogenome phylogenies and reveals the appearance of the MRCA of the *U. crassus* complex clade during the Miocene, around 20 MYA (Fig. 5). Diversification began in the Early Miocene with the divergence of species from southern Europe and Anatolia, i.e. *U. tumidiformis*, *U. sesirmensis*, *U. desectus*, *U. damascensis*, and *U. ionicus.* Species from higher latitudes diverged in the Pliocene (Fig. 5), except for the splits between *Unio carneus* from the Ohrid and Buna basins in the Balkans and the widespread *U. nanus*, between the Anatolian *U. bruguierianus* and *U. mardinensis*, and between *U. crassus* s. str. and the Caucasian *U. gontierii,* which appear to be more recent, i.e. Late Pleistocene.

3.7.2. Anchored Hybrid Enrichment

The time-calibrated AHE phylogeny shows an almost identical topology to the BI and ML AHE phylogenies (Fig. 5). All branches are well supported and show the appearance of the MRCA of the *U. crassus* complex clade during the Miocene approximately 20 MYA (Fig. 5). Diversification started at the beginning of the Miocene with the divergence of species from southern Europe, the Iberian *U. tumidiformis*, the southwestern Balkan *U. ionicus* + *U. carneus*, and the Anatolian and Levantine *U. sesirmensis* + *U. damascensis*. The remaining species diverged in the second half of the Miocene (Fig. 5). The western Balkan *U. carneus* and *U. ionicus*, the eastern Balkan *U. vicarius*, and *U. desectus* and the widespread northern species *U. crassus* s. str. and *U. nanus* represent more recent divergences, occurring around 10 MYA (Fig. 5).

3.8. Comparison of mitochondrial and nuclear phylogenies

The phylogenies based on AHE and mtDNA topologies revealed incongruent patterns in a few nodes indicating mito-nuclear discordance in three pairs of species (see Figs. 4-5). According to the AHE phylogenies, *U. gontierii* is more closely related to its southern neighbour *U. mardinensis* (see Figs. 4-5), whereas according to the mtDNA phylogenies, *U. gontierii* and its northern neighbour *U. crassus s. str.* are sisters (see Figs. 4-5). In the AHE phylogeny, *U. mardinensis* and *U. bruguierianus* do not cluster together, but their mtDNA sequences are closely related (see Figs. 4-5). Additionally, *U. carneus* clusters with *U. ionicus*, its southern neighbour, in the AHE phylogeny, but with *U. nanus*, its northern neighbour, in the mitochondrial phylogeny (see Figs. 4-5).

3.9. Morphometric analyses

The first two PC-axes generated from the 18 Fourier coefficient dataset explain 19% and 17% of the overall variation in the dataset, respectively (Fig. 6). Species of the *U. crassus* complex differ significantly from each other in both PC1 and PC2 (ANOVAs: PC1: df =11, 534, F=7.792, P<0.0001; PC2: df =11, 534; F=8.215, P<0.0001). Tukey's *posthoc* pairwise comparisons reveal that PC1 values differ between (1) *U. damascensis* and all other species except *U. carneus*, and (2) *U. carneus* and *U. bruguierianus*, *U. crassus* s. str., *U. nanus* and *U. mardinensis*, respectively (Table 2). However, a broad morphospace overlap is observed between several species of the *U. crassus* complex, resulting in difficulties in using shell shape features to distinguish the various cryptic species. The scatterplot and synthetic outlines along PC1 (Fig. 6) indicate that *U. damascensis* and *U. carneus* tend to be more wedge-shaped than (most) other species of the *U. crassus* complex, which tend to have a straighter, sometimes convex ventral margin. Significant differences in PC2 values were found (1) between *U. carneus* and all other species except *U. damascensis*, *U. mardinensis* and *U. tumidiformis*, (2) between both *U. damascensis* and *U. bruguierianus* and *U. crassus* s. str., *U. desectus*, *U. gontierii* and *U. vicarius*, respectively, and (3) both *U. mardinensis and U. nanus* and *U. gontierii*, respectively. These results indicate that *U. carneus*, *U. damascensis* and *U. bruguierianus* tend to exhibit shorter, more oval shells, whilst *U. gontierii*, *U. desectus*, *U. vicarius* and *U. crassus* s. str. tend to have comparatively elongated shells (Fig. 6).

Pairwise comparisons across the whole dataset reveal a similar pattern (ANOSIM: R = 0.1636, p < 0.0001), with *U. carneus* outlines being different from all but one species (*U. tumidiformis*), *U. damascensis* being different from all but two species (*U. sesirmensis* and *U.*

tumidiformis), and *U. mardinensis* being different from all but three species (*U. desectus*, *U. ionicus*, *U. tumidiformis*) (Table 2). All other species do not show a significant difference from at least four other *Unio* species, respectively.

Finally, discriminant analysis on the morphometric dataset confirms that variation in shell shape does not allow direct assignment of *U. crassus* complex specimens to the correct species. Shell contour morphometric assignments agree with genetic assignments in only 45% of the specimens. The proportion of correct assignments is high for *U. desectus* (82% jackknifed), *U. tumidiformis* (80%, but note low replicate number), *U. carneus* (75%), medium for *U. damascensis* (67%), *U. mardinensis* (67%), *U.* sesirmensis (60%) and *U.* gontierii (58%), and low (<50%) for all other species. The most commonly confused species-pairs are *U. bruguierianus* - *U. ionicus* (average 13% in both directions), *U. crassus* s. str. - *U. nanus* (13%), *U. mardinensis* - *U. vicarius* (13%), and *U. damascensis* - *U. vicarius* (11%). None of these four pairs are sister species in the mitogenome phylogeny, whereas only *U. crassus* s. str. and *U. nanus* are sister species in the AHE phylogeny.

3.9. Distributions, genetic diversity and phylogeography

The geographical extent of the *U. crassus* complex lineages, recognised here as species (Table 3), varies in size, with only two species, *U. crassus* s. str. and *U. nanus*, being widespread in northern and central Europe, and the remaining 10 species occurring in more restricted distributions in southern regions of Europe and western Asia (Fig. 1). All species are allopatric, with three exceptions: first, the most widespread *U. crassus* s. str. and *U. nanus* overlap in most of the distribution of *U. nanus*, except in the Rhone basin (Fig. 1); second, both of these species also overlap with the northern range of *U. vicarius* in the lower Danube basin (Fig. 1); and third, *U. crassus* s. str. overlaps with *U. bruguierianus* in the coastal basins of the Black Sea, south of the Danube basin (Fig. 1). Species occurred in a single (*U. carneus* and *U. sesirmensis*) up to 27 independent river basins (*U. crassus* s. str.) (Fig. 1; Table 3). The number of COI haplotypes per species ranges from 5 for the Asian species *U. mardinensis* and *U. sesirmensis* to more than 30 for *U. nanus* (31) and *U. crassus* s. str. (33) (Table 3). Genetic diversity (haplotype diversity) ranges from 0.437 for the southern Balkan range-restricted species *U. ionicus* to 0.896 for the Eurasian *U. bruguierianus*. Phylogeographic structure is generally related to the number of separate river basins occupied by a species and is generally lower for more restricted-range species such as *U. desectus* or *U. tumidiformis* (see Discussion). Distributions and species-specific phylogeographic patterns are described in more detail in the Discussion section.

3.10. Taxonomy and systematics

The *U. crassus* complex is here divided into 12 species. Given the large number of existing synonyms of *U. crassus*, all molecular lineages detected here correspond to an available nominal species. Following Haas (1969), we have applied the names *U. crassus* s. str. and *U. nanus* to those lineages with distributions corresponding to the subspecies *Unio c. crassus* and *Unio c. cytherea* of Haas (1969). The remaining species names, reinstated here from the *U. crassus* synonymy, were assigned from the available older names for which the type locality matched or was within the range of the corresponding collected and sampled specimens. We provide a full synonymy of nominal taxa for the *U. crassus* complex in Sup. Appendix 2.

4. DISCUSSION

Based on the integrative phylogenetic, phylogeographic and morphometric dataset of the *U. crassus* complex across its range, we propose a revised taxonomy that accounts for previously unrecognised cryptic diversity, particularly in the southeastern range. This study also shows the importance of contrasting and combining information from nuclear and mitochondrial genes to define species boundaries and resolve the phylogenetic and phylogeographic relationships among species.

4.1. Lack of complete mito-nuclear coherence

As expected, our results show that it is necessary to include a wide range of nuclear and mitochondrial markers to resolve the evolutionary history of morphologically cryptic lineages. Our COI-based molecular species delimitation methods and associated phylogenies supported the recognition of 10 species-level lineages in the *U. crassus* complex, whereas 12 species-level lineages were supported using AHE data (Figs. 2 and 4). The topologies of the mtDNA-based phylogenies also differ from those generated using AHE data, with the latter showing an evolutionary pattern more consistent with the geographic distribution of the species. (Figs. 2 and 4). Examples include the clustering in the AHE phylogenies of the two adjacent southwestern Balkan species *U. carneus* and *U. ionicus*, the central and southern Asian species *U. sesirmensis* and *U. damascensis*, the three Anatolian and Caucasian species *U. bruguierianus*, *U. mardinensis*, and *U. gontierii*, the two species from central-eastern Greece *U. vicarius* and *U. desectus*, and finally the two widespread and northern European species *U. nanus* and *U. crassus* s. str. (Figs. 2-4). Mito-nuclear discordance was detected in three pairs of species. In the AHE phylogeny, *U. gontierii* is more closely related to its southern neighbour *U. mardinensis* (Figs. 3-5), whereas in the mtDNA phylogenies, *U. gontierii* and its northern neighbour *U. crassus* s. str. are sisters with low genetic divergence (1.1% COI uncorrected *p*-distance) (Figs. 2-5; Table 1). A similar situation occurs between *U. mardinensis* and *U. bruguierianus*, which do not directly cluster together in the AHE phylogeny but show closely related mtDNA sequences with low genetic divergence (1.3% COI uncorrected *p*-distance) (Figs. 2-5; Table 1). Finally, *U. carneus* clusters with its southern neighbour *U. ionicus* in the AHE phylogeny but with its northern neighbour *U. nanus* in the mitochondrial phylogeny (Figs. 2, 4-5). In the species pair *U. carneus* - *U. nanus*, the mtDNA divergence is higher (3.1% COI uncorrected *p*-distance) than between the other two species pairs previously mentioned (Table 1). These patterns could be explained by ancient introgression events between *U. crassus* s. str. + *U. gontierii* and *U. mardinensis* + *U. bruguierianus* during the Pleistocene and a similar but older Pliocene introgression event between *U. carneus* and *U. nanus*. Alternatively, incomplete lineage sorting may account for the high degree of similarity of *U. gontierii* and *U. crassus* s. str. mtDNA. These patterns of genetic connectivity and gene flow around the Black Sea during the Pleistocene have been reported for freshwater fishes (Kotlík et al., 2003) and can be explained by the considerable salinity fluctuations of the Black Sea since its formation, with long periods when it was predominantly freshwater (Ryan et al., 2003; Riboulot et al., 2018). The close relationship of the mtDNA of *U. carneus* with the neighbouring *U. nanus* can also be explained by an older (Pliocene) introgression of *U. nanus* mtDNA in *U. carneus* populations (Figs. 2-4). Pliocene exchanges between the faunas of the Danube Basin and Ohrid Lake have been reported for fishes using genetic divergence dating (Perdices et al., 2007; Šedivá et al., 2008). In freshwater mussels, strong discordance between mtDNA markers and nuclear microsatellite data had already been shown by Chong et al. (2016) in populations of the North American genus *Cyprogenia*, where genetic clusters varied in number and composition depending on the marker. Discordance between mitochondrial and nuclear data has also been reported from *Sinanodonta* populations in Japan, providing evidence for mitochondrial introgression (Sano et al., 2022) and challenging mtDNA-based species delineations (Lopes-Lima et al., 2021).

Due to the detection of distinct mtDNA and nuclear genome evolutionary patterns, a combination of whole mitogenomes and AHE proved essential for species delimitation in the *U.*

crassus complex and may be useful in other freshwater mussel groups, but a detailed study with AHE/mtDNA sequence data from more specimens is still needed to fully unravel their unique evolutionary history.

4.2. Biogeography and phylogeny of the U. crassus complex

The biogeography of the *U. crassus* complex follows a classic European biogeographic pattern, with high species diversity and more restricted ranges in the south, contrasting with low species diversity and widespread ranges in the north (Weiss and Ferrand, 2007). These southern lineages with restricted ranges are thought to occur in Pleistocene glacial refugia, whereas the northern areas are generally occupied by postglacial expansions of a single lineage. The multiple species found in the Balkans and Anatolia reflect a pattern of 'refugia within refugia' (Goméz and Lunt, 2007) and highlight the complex geological history of the region (Froufe et al., 2016; Lopes-Lima et al., 2021 and references therein). This pattern was not observed in Iberia where a single refugium was detected for *U. tumidiformis*, which displays low genetic geographic structure (Fig. 1), in contrast to another freshwater mussel species (e.g. *Anodonta anatina*) with a marked phylogeographic structure comprising multiple lineages within this region (Froufe et al., 2014; Lopes-Lima et al., 2016). In freshwater mussels, the Italian peninsula and the Adriatic coast of the northern Balkans again show a unique fauna, with the absence of species from the *U. crassus* complex (Froufe at al., 2017; Riccardi et al., 2020).

The most recent common ancestor of *Unio* most likely arrived from Asia via the coastal basins of the proto-Paratethys Sea, which existed in Central Asia during the Paleogene (Kaya et al., 2019, 2020). Our time-calibrated phylogenies indicate that diversification of the main groups of *Unio*, i.e. the *tumidus*, *gibbus*, *pictorum* and *crassus* clades, most likely occurred in the Late Eocene, or less likely in the Middle Eocene or Oligocene (Fig. 5). The final split between the *crassus* and *pictorum* clades occurred in the Oligocene or Early Miocene, most likely in the Late Oligocene (Fig. 5).

Within the *crassus* clade, i.e. the *U. crassus* complex, all AHE phylogenies including flanking region loci are well-supported in all branches and are consistent with patterns of geographic proximity among the different species. These results highlight the utility of the conserved AHE probe set, together with its variable flanking regions, for estimating intrageneric shallow phylogenies (Figs. 4-5), as previously shown by Smith et al. (2020). All target region + flanking AHE phylogenies show that diversification within the *U. crassus* complex began with the split of the Iberian species *U. tumidiformis*, followed by two further divergence events, one containing the adjacent southwestern Balkan populations (*U. ionicus* and *U. carneus*) and the other involving the central Anatolian and Levantine populations (*U. sesirmensis* and *U. damascensis*). This phylogeny indicates a Mediterranean origin for the MRCA of the *U. crassus* complex during the Early Miocene, which then established and diverged in Iberia, the southwestern Balkans, and Anatolia (Figs. 4-5). This pattern is very similar to that observed in the freshwater mussel genus *Potomida* for the three currently recognised species, which first appeared in the same locations, i.e. one in Iberia, one in the southwestern Balkans, and one in southern Anatolia and the Middle East, during the same period (Froufe et al., 2016; Araujo et al., 2017).

4.3. Taxonomy and species delineation

Following the synopsis by Haas (1969), which integrated 235 previously described *Unio* taxa into *U. crassus*, six *Unio* species were resurrected from the synonymy based on morphological, geographical and mitochondrial data (*U. tumidiformis*: Reis and Araujo, 2009; *U.*

bruguierianus and *U. ionicus*: Araujo et al., 2018; *U. carneus*: Lyubas et al., 2022; *U. damascensis* and *U. sesirmensis*: Lopes-Lima et al., 2021). Here we restore five additional nominal taxa to species, i.e. *Unio desectus* **stat. rev.**, *Unio gontierii* **stat. rev.**, *Unio mardinensis* **stat. rev.**, *Unio nanus* **stat. rev.**, and *Unio vicarius* **stat. rev.** All species recognised here represent divergent genetic units, as shown by nuclear genetic data and most also by mitochondrial data. However, as discussed above, incongruence between mtDNA and nuclear DNA was observed in three pairs of species, probably reflecting ancient introgression and/or incomplete lineage sorting. This incongruence is evident from the results of the COI species delimitation analyses, which coherently separated the *U. crassus* complex into only 10 evolutionary lineages (Fig. 2). The remaining two species are supported by the AHE phylogeny, which has a broad genomic representation and a clear agreement of species entities with geographic distributions.

Morphometric results show that the shell outline was generally a poor predictor of species entities in the *U. crassus* complex and regularly failed to assign specimens to the correct species (i.e. only 45% correctly assigned specimens). Nevertheless, species assignments were higher for species with deeper phylogenetic splits within the *U. crassus* complex (particularly *U. carneus*, *U. damascensis*, *U. bruguierianus* and *U. tumidiformis*). Although the shell outline was not completely discriminative in species identification, some morphological characters can be used to separate some species (see below). Furthermore, more than half of the species recognised here were already distinguished into different subspecies by Haas (1969). Although this author only separated the different *U. crassus* subspecies using qualitative morphological descriptions, the degree of agreement with the genetic data observed here is remarkable (Fig. 1). For example, the distributions of *U. ionicus*, and *U. carneus* show almost perfect agreement with Haas' (1969) observations (Fig. 1). The same is true when considering the extensive overlap of *U. nanus* with the subspecies *Unio crassus cytherea* (which we currently synonymise with *U. nanus*; Sup. Appendix 2) as presented by Haas (1969) (Fig. 1). Two additional species, i.e. *U. tumidiformis* and *U. gontierii*, were placed in separate subspecies by Haas (1969), although the author's description of their spatial distributions does not fully agree with those resolved in the present study based on molecular data (Fig. 1). The lack of a clear morphological distinction may also be due to possible hybridisation, especially in sympatric species. Hybridisation between *U. nanus* and *U. crassus* s. str. has already been suggested in a study of female and male mtDNA lineages in Poland (Mioduchowska et al., 2016). In the future, it will be important to study the contact zones and areas of distributional overlap among species in more detail. Such studies can be achieved by using more genomic data and tailored sampling efforts.

4.4. The 12 valid species within the U. crassus *complex*

The following section provides a brief overview of the 12 taxa accepted here as valid species, including a synopsis of their taxonomy, phylogeny, genetic diversity, and distribution, as well as the main arguments for the validity of each taxon as a species and a short outline of conservation considerations. It should be noted that the number of individuals sequenced per population was not high enough to allow phylogeographic statistical tests, and therefore the phylogeographic observations are mainly descriptive. Unreferenced conservation remarks are based on observations by the authors of the study.

Unio bruguierianus Bourguignat, 1853

Taxonomy: Described by Bourguignat in 1853 from Smyrna, western Anatolia, Türkiye, this species was considered by Haas (1969) to be a subspecies of *U. crassus*, i.e. *U. crassus bruguierianus*, comprising populations from eastern Greece, all of Anatolia, and the Middle East. Based on mitochondrial data, *U. bruguierianus* was erected from the synonymy of *U. crassus* by

Araujo et al. (2018), albeit for populations of the lower Axios and Pinios Rivers, which are revived in this study as *Unio desectus* (see below). More recently, based on similar markers but more extensive sampling in Türkiye, *U. bruguierianus* was revised to occur in Thrace, eastern Greece to European Türkiye, and western Anatolia, with the central to southern Anatolian and Levantine populations being reassigned to two other species, namely *U. sesirmensis* and *U. damascensis* (Lopes-Lima et al., 2021). Lopes-Lima et al. (2021) considered the Arax and upper Euphrates populations (here revived as the valid species *U. mardinensis* **stat. rev.**) to be part of *U. bruguierianus* due to the confounding effects of the mtDNA introgression between *U. mardinensis* **stat. rev.** and *U. bruguierianus*.

Phylogeny & genetic diversity: In the AHE phylogenies, this species is sister to its geographical neighbours *U. mardinensis* + *U. gontierii* (Figs. 4-5), and together these three species are sister to a clade containing all species from the northernmost regions of Europe (Figs. 4-5). The phylogenetic position of *U. bruguierianus* in the mitogenome phylogenies clusters with *U. mardinensis* inside a clade containing *U. carneus*, *U. nanus*, and *U. vicarius* (Figs. 4-5). *Unio bruguierianus* has an interesting phylogeographic structure with an Asian haplogroup (haplotypes 10-17: Fig. 7) that is quite distinct from the other haplotypes, which are mostly from Europe although some are Asian. This structure suggests an initial separation of European and Asian haplotypes, followed by one or more gene flow events between Asian and European populations across the Sea of Marmara, which has fluctuated in salinity between fresh and brackish for long periods up to the Pleistocene (Lopes-Lima et al., 2021). The species has the highest haplotypic diversity of all species in the *Unio crassus* complex and the highest intraspecific divergence between haplotypes (Table 3).

Distribution: Occurs in the western Anatolian region of Türkiye, north of the Büyük Menderes and west of the Sakarya River basins. Its distribution extends to the Aegean and Black Sea river basins of European Türkiye, Greece (east of the Kompsatos River basin), and Bulgaria (Maritsa River basin and Black Sea coastal basins south of the Kamchiya River basin) (Figs. 1 and 7).

Diagnosis: *Unio bruguierianus* represents a unique genetic lineage in both the nuclear and mitochondrial genomes, except for observed mitochondrial introgression with *U. mardinensis*, which results in a low genetic distance between both in COI. *Unio bruguierianus* has shells with an antero-posteriorly shorter outline than most of the other species and it has an oval shape, although it is very difficult to distinguish from most other species in this complex based on shell shape alone (Fig. 6; Tables 2 and S4). It is also allopatric to its closer genetic relatives *U. crassus* s. str., *U. gontierii*, *U. mardinensis*, and *U. vicarius* (Fig. 1; Table 1).

Conservation: There are no ongoing monitoring programmes or conservation plans for this species and population trends have not been quantified. However, the species' range is severely fragmented by dams and other physical barriers, and its populations are declining significantly. Anatolian populations are threatened by river channelling, poor river management and pollution. In the Aegean, the species is severely threatened by pollution, water scarcity and hydromorphological changes, and documented populations have low densities and highly localised distributions. Populations in the coastal rivers of the Black Sea appear to be in better condition but are severely threatened by drought and water abstraction. Little is known about their ecology and life history traits. Due to its sympatry with other species within the complex in the coastal basins of the Black Sea, live specimens of *U. bruguierianus* collected from these basins for use in potential future conservation actions such as propagation and/or translocation should be subjected to molecular testing to ensure accurate species identification.

Unio carneus Küster, 1854

Taxonomy: Described by Küster in 1854 for specimens from tributaries of the Morača River (Skadar Lake Basin) in Montenegro, it was considered by Haas (1969) to be a subspecies of *Unio crassus*, i.e. *U. crassus carneus*, including populations from the Skadar Lake Basin. Based on mitochondrial data, the species was resurrected from the *U. crassus* synonymy by Lyubas et al. (2022) with the same distribution. Here we extend this distribution to the entire Drin River basin, including both the Ohrid and Skadar basins (Fig. 1).

Phylogeny & genetic diversity: The species has incongruent positions in the mitochondrial and nuclear phylogenies (Figs. 2, 4-5). In the nuclear phylogeny, it clusters with its southern neighbour *U. ionicus*, representing one of the earlier divergence events of the complex (Figs. 4-5). However, in the mitochondrial phylogenies, it is closer to its northern neighbour *U. nanus*, possibly reflecting ancient gene flow events between these two species (Figs. 2, 4-5). *Unio carneus* does not show a strong genetic structure, although unique haplotypes support some differentiation between Lake Ohrid, and the lower Drin River basin (including Lake Skadar) (Fig. 8).

Distribution: The species occurs exclusively in rivers and lakes within the Drin River basin in Montenegro, Albania, and North Macedonia, including the Crnojevića and Zeta Rivers, tributaries of Lake Skadar in Montenegro, the streams and channel networks of the lower Drin River in Albania, and the Lake Ohrid watershed (Figs. 1 and 8).

Diagnosis: The species represents a unique divergent genetic lineage in both the nuclear and mitochondrial genomes (Figs. 2, 4-5). In shell outline, this species is similar to *U. bruguierianus* and the southern Anatolian *U. damascensis*, with short and oval shells and a wedge-shaped posterior region. It is restricted to one large basin and is allopatric to all other species within the *U. crassus* complex (Fig. 1).

Conservation: The species is declining as a result of habitat degradation and hydromorphological changes, particularly those caused by dams. Little is known about its ecology and life history traits.

***Unio crassus* s. str.** Philipsson in Retzius, 1788

Taxonomy: This species was described by Philipsson in Retzius in 1788 from specimens found in European rivers. Although the type specimens are lost and of uncertain geographical origin, they were most likely from northern Europe, where these authors worked and lived. This situation was recognised by Haas (1969), who considered the subspecies *Unio crassus crassus* to occur in north-eastern Europe (Fig. 1). We followed Haas (1969) and considered the north-eastern lineage to be *Unio crassus* sensu stricto (Fig. 1). Prié and Puillandre (2014) named this lineage *Unio crassus courtillieri* because it is the only lineage found in the Loire River (Fig. 1, bottom), and the earliest name that applied to the Loire populations was *Unio courtillieri* (type locality = 'ruisseau de Jarrie', a tributary of the Loire). Here we synonymise *Unio courtillieri* with *Unio crassus s. str.* (Sup. Appendix 2).

Phylogeny & genetic diversity: The mitochondrial and nuclear phylogenies do not agree on the position of *U. crassus* s. str. (Figs. 2-4). *U. crassus* s. str. clusters with *U. nanus* in the nuclear phylogeny and with *U. gontierii* in the mitochondrial phylogeny. Whereas the nuclear phylogeny suggests a closer relationship between the two widespread and northern species with a largely overlapping distribution, the mitochondrial phylogeny suggests a Pleistocene hybridisation event between *U. crassus* s. str. and *U. gontierii* (Figs. 1-4). No clear phylogeographic structure was detected for *U. crassus* s. str., but the higher number of haplotypes from the Danube may suggest that the origin of the species lies somewhere in the lower sections of this basin (Fig. 9). This

hypothesis should be tested in the future with further sampling of more individuals and populations coupled with sequencing and phylogeographic inference.

Distribution: *Unio crassus* s. str. is restricted to Europe, occurring in most Atlantic and Baltic SeaZ river basins from France to Russia, including Sweden and Finland. It is also present in river basins in Eastern Europe extending to the Caspian and Black Sea basins, from the Danube to the Ural basins (Figs. 1 and 9).

Diagnosis: The species represents a unique genetic lineage in both the nuclear and mitochondrial genomes, except for the mitochondrial introgression with *U. gontierii*, and therefore both have a low genetic distance in this marker (Table 1). The species overlaps with *U. nanus* in most of its western range and with *U. vicarius* and *U. bruguierianus* in its south-central range (Fig. 1). Because of its shell morphological plasticity and wide distribution, it is very difficult to distinguish *U. crassus* s. str. from other species in the complex using only shell morphological characters (Tables 2 and S4).

Conservation: Throughout its distribution, the number of populations and individuals has decreased significantly, and *U. crassus* s. str. is now considered highly threatened in several European countries (Lopes-Lima et al., 2017b). Previously published studies on the ecology, biology and conservation of the species did not distinguish it from *U. nanus* and should be re-evaluated within the new species concept presented here. As this species is also the subject of an increasing number of captive breeding efforts and reintroductions (Geist et al., in press), live specimens of *U. crassus* s. str. to be used for future potential conservation actions such as propagation and/or translocation should be subjected to molecular testing to ensure accurate species identification.

Unio damascensis Lea, 1863

Taxonomy: This species was described by Lea in 1863 from a specimen collected near Damascus, Syria, in the same publication as two other species, *U. orontesensis* Lea, 1863 and *U. syriacus* Lea, 1863, all of which were synonymised by Haas (1969) as *Unio crassus bruguierianus*. Following the principle of the first reviser (Article 24.2 of the International Code of Zoological Nomenclature), Falkner (1994) gave priority to *U. damascensis*, and this name was retained and resurrected from the *Unio crassus* synonymy in a recent molecular study of freshwater mussels of the eastern Mediterranean (Lopes-Lima et al., 2021).

Phylogeny & genetic diversity: *Unio damascensis* clusters with its northern neighbour *U. sesirmensis* in the nuclear phylogeny, whereas support for its placement in the mitochondrial phylogenies is unclear (Figs. 2, 4-5). The species has a distinct spatial genetic structure, with individuals from each major river basin having unique haplotypes (Lopes-Lima et al., 2021). The phylogeographic patterns and distribution of this species have been described in more detail by Lopes-Lima et al. (2021) and are therefore not depicted here.

Distribution: This species occurs in southern Anatolia, in the Tarsus, Ceyhan and then south to the Orontes River basin in Türkiye and Syria (Fig. 1; Lopes-Lima et al., 2021).

Diagnosis: This species is represented by a unique genetic lineage in both the nuclear and mitochondrial genomes (Figs. 2-4). *Unio damascensis* is allopatric with all other species within the *U. crassus* complex (Fig. 1). Shells of this species are shorter antero-posteriorly and more wedge-shaped posteriorly than those of most species (Fig. 6, Tables 2 and S4).

Conservation: Almost all the small coastal basins of Syria and southern Türkiye are now either dry and/or highly polluted. The Orontes River basin is also highly polluted and eutrophic. Most

rivers and streams in the area are threatened by increasing agricultural pressure (Lopes-Lima et al., 2021). As a result, we believe that the number of populations and effective population sizes of *U. damascensis* are declining substantially, making this a priority species for conservation.

Unio desectus Westerlund in Westerlund & Blanc, 1879 **stat. rev.**

Taxonomy: The species was described by Westerlund in 1879 from specimens collected in the Pinios River near Volos, Greece. It was then considered by Haas (1969) to be a junior synonym of *U. crassus bruguierianus*. The divergence of the mitochondrial sequences of specimens from the lower Pinios and Axios from other species in the *U. crassus* complex was first noted by Araujo et al. (2018), who resurrected the species as *Unio bruguierianus*. However, more recent molecular analyses of *Unio* populations from the eastern Mediterranean (Lopes-Lima et al., 2021) reassigned the species *U. bruguierianus* to Turkish and western Greek populations and did not include the highly divergent sequences previously published by Araujo et al. (2018) from the Pinios and Axios, which we now include in *U. desectus* **stat. rev.**

Phylogeny & genetic diversity: In the AHE phylogenies, *U. desectus* is sister to the neighbouring *U. vicarius*, but in the mitogenome phylogenies it is positioned more basally, as sister to a clade containing *U. carneus*, *U. nanus*, *U. vicarius*, *U. bruguierianus*, *U. crassus* s. str., and *U. gontierii* (Figs. 4-5), whereas in the COI phylogeny, it is even more basal (Fig. 2). The lack of a coherent genetic geographic structure suggests a recent separation of the lower sections of the three basins, which were probably connected until the last glaciation (Zogaris and Economou, 2017) (Fig. 10).

Distribution: The species occurs exclusively in the lower reaches of the Aliakmonas, Axios, and Pinios rivers in eastern mainland Greece, and thus has a very restricted distribution (Figs. 1 and 10).

Diagnosis: This species is represented by a unique genetic lineage in both the nuclear and mitochondrial genomes (Figs. 2-4). The species is mostly parapatric with *U. vicarius* in the middle reaches of the Aliakmonas and Pinios basins, although there may be an overlap in the lower Aliakmonas where a specimen of *U. vicarius* was found (Fig. 1; Table S1). The shell shape is quite distinctive as shown by the discriminant analysis with a high proportion of correct assignments (82%), and it can be distinguished from *U. vicarius* by being antero-posteriorly compressed, posteriorly shorter, and more oval (Tables 2 and S4).

Conservation: Only three populations occur in the lower reaches of the Aliakmonas, Axios, and Pinios rivers in central-eastern Greece, making conservation of this species a key priority. Populations are severely fragmented by dams, weirs, and other physical barriers and are thought to be declining as a result of this fragmentation, combined with ongoing degradation of habitat quality caused by intensification of irrigated agriculture, infrastructure development, poor river management, and physical alteration of substrate (i.e. flood control works, sand, and gravel extraction) and water quality. Due to its sympatry with *U. vicarius*, live specimens of *U. desectus* to be used for future potential conservation actions such as propagation and/or translocation should be subjected to molecular testing to ensure accurate species identification.

Unio gontierii Bourguignat, 1856 **stat. rev.**

Taxonomy: The species was described by Bourguignat in 1856 based on specimens from the Chorna River in Crimea. It was subsequently synonymised with *U. crassus* by Haas (1969) as *U. crassus gontierii* for populations in the Caucasus, and the basins of the Kura River and Russian and Georgian rivers between the Black and Caspian Seas.

Phylogeny & phylogeography: *Unio gontierii* clusters with its southern neighbour *U. mardinensis* in the AHE phylogenies (Figs. 4-5). However, it groups with its northern neighbour *U. crassus* s. str. in the phylogenies based on mtDNA, suggesting a more recent genetic exchange or the retention of an ancient polymorphism (Figs. 2, 4-5). This species shows a spatial genetic structure that reflects the locations of the river basins in which it occurs, with unique haplotypes in several rivers, particularly those at the edge of the sampled distribution (Fig. 11).

Distribution: The species is thought to occur in rivers and streams draining into the Black Sea from Crimea to Georgia and in the Kura River basin (excluding the Arax River) draining into the Caspian Sea (Figs. 1 and 11). However, its presence in the proposed western range of the species in Crimea is based only on data from Haas (1969) and should be confirmed in the future. In the absence of molecular data, the occurrence of *U. gontierii* in the rivers of the eastern and the south-eastern Greater Caucasus draining into the Caspian Sea and in the lower Kura River also needs to be confirmed. These areas are likely to be occupied either by *Unio gontierii*, by *U. mardinensis* which occurs in the Arax River basin (a major southern tributary of the Kura River), or by both.

Diagnosis: This species is represented by a unique genetic lineage in both the nuclear and mitochondrial genomes, although the latter is closely related to *U. crassus* s. str. as explained above (Figs. 2, 4-5). It is very difficult to distinguish *U. gontierii* from other species in the complex using only shell morphological characters, although it is generally more elongated than most other species (Table 2). The species appears to be allopatric with all others in the *U. crassus* complex and parapatric with *U. mardinensis* at the Kura/Arax rivers interface, but specimens from Crimea and the middle and lower reaches of the Kura River basin need to be molecularly analysed to better understand the range of *U. gontierii*.

Conservation: The species is highly threatened and declining rapidly as rivers in the Crimea are affected by dams and pollution. The problem is thought to be no less acute in Georgia but is little known. Extensive damming for hydroelectric power (Japoshvili et al., 2021), pollution, and illegal electrofishing are the main problems affecting freshwater biodiversity in Georgia, including mussels. As the recent (i.e. last 50 years) distribution or population trends have never been studied for any mussel species in Georgia, the conservation status is not assessed for any of these species. Protected areas in Georgia, which are mostly established for terrestrial ecosystems, do not exceed 10% of the country's territory and are therefore less likely to provide habitat protection for freshwater unionids. Therefore, the conservation status and challenges of *U. gontierii* need to be assessed throughout its range.

Unio ionicus Drouët, 1879

Taxonomy: The species was described by Drouët in 1879 from specimens found in drainage ditches on the island of Lefkada in western Greece. The species was considered by Haas (1969) to be one of the *U. crassus* subspecies, namely *U. crassus jonicus* [sic], including populations from western mainland Greece and the islands of Lefkada and Corfu. It was subsequently erected by Araujo et al. (2018) from the synonymy of *U. crassus* as the valid species *U. ionicus*.

Phylogeny & genetic diversity: *Unio ionicus* diverged early in the evolutionary history of the *U. crassus* complex and is clustered with its northern neighbour *Unio carneus* in the nuclear phylogenies (Figs. 3-4). The species has low genetic diversity with no clear structure but with unique haplotypes in Albania and the Peloponnese rivers (Fig. 12; Table 3).

Distribution: *Unio ionicus* occurs only in rivers along the western coast of the southern Balkans, from the River Bistrices in southwestern Albania to the River Pamisos in the Peloponnese, Greece (Figs. 1 and 12). It was also historically present on the Ionian islands of Corfu and Lefkada, but no recent surveys have confirmed its current presence on these islands.

Diagnosis: This species is highly divergent from other species in the *U. crassus* complex in both the nuclear and mitochondrial genomes (Figs. 2-4). The species is endemic to the southwestern river basins of the Balkans within the Ionian ecoregion of Greece and is allopatric with other members of the *U. crassus* complex. It is very difficult to distinguish *U. ionicus* from other species in the complex by shell outline alone, especially from *U. bruguierianus* (Tables 2 and S4).

Conservation: The distribution of this species is poorly known and should be updated based on the species identification methods presented here. In the Pamisos River, much of the population has been extirpated due to river engineering, wetland drainage, urban sprawl and water abstraction. The remaining populations are also declining and face similar threats, although there is no hard data on population trends.

Unio mardinensis Lea, 1865 **stat. rev.**

Taxonomy: This species was described by Lea in 1865 together with two other species in the same publication, i.e. *Unio orphaensis* Lea, 1865 and *Unio kullethensis* Lea, 1865 for specimens collected in the upper Tigris near Mardin in south-eastern Türkiye. This species was considered by Haas (1969) to be part of *Unio crassus bruguierianus* based on morphological and geographical arguments. More recently, it has been considered a junior synonym of *U. bruguierianus* based on the same arguments, and COI data (Lopes-Lima et al., 2021). Here, we resurrect this species from the synonymy of *U. bruguierianus*, giving priority to the name *Unio mardinensis* Lea, 1865 according to the first reviser principle (Article 24.2 of the International Code of Zoological Nomenclature).

Phylogeny & genetic diversity: The nuclear and mtDNA phylogenies show distinct topologies, with the former clustering *U. mardinensis* as sister to *U. gontierii*, whereas in the latter *U. mardinensis* haplotypes are nested within *U. bruguierianus*, suggesting probable introgression or incomplete lineage sorting (Figs. 2-4). This species was sampled from a very limited area within its potential range, but the few populations that were sampled show a slight separation between the Euphrates and Arax haplotypes (Fig. 13). COI haplotype diversity is higher in the Euphrates than in the Arax, where only a single haplotype was detected (Fig. 13).

Distribution: *Unio mardinensis* occurs in the Arax basin (so far not known from the Kura River), the upper Euphrates, and is expected to occur also in the upper Tigris and Van Lake basins (Figs. 1 and 13), but this needs to be confirmed with molecular data.

Diagnosis: The species has unique haplotypes in both the nuclear and COI lineages, although the COI haplotypes have low genetic diversity and are nested within *U. bruguierianus* as discussed above (Table 3). Morphometrics showed that *U. mardinensis* has a moderately distinctive shell contour, with approximately 70% of correct species assignments based on shell morphology (Table 2). The species has an exclusive distribution in the Tigris and Euphrates basins and a parapatric distribution to *U. gontierii* in the interface between the Arax and Kura rivers (Figs. 1, 11 and 13).

Conservation: Very little is known about the conservation status of the species, but streams in the area are severely threatened by desiccation and eutrophication due to agricultural intensification, and large rivers have been severely fragmented by dams. Given the limited area where recent populations have been found, it is thought that the species has declined significantly in recent decades due to habitat loss and degradation.

Unio nanus Lamarck, 1819 **stat. rev.**

Taxonomy: This species was described by Lamarck in 1819 based on a specimen from the Franche-Comté region of France. The species was considered by Haas (1969) to be a synonym of *U. crassus batavus* and distinct from the subspecies *U. crassus cytherea*, but because of the overlap in distribution between these two nominal taxa in the Rhône basin, where a single molecular lineage was found, we synonymise *U. cytherea* and all nominal taxa recognised by Haas (1969) under *U. crassus cytherea*, with *U. nanus*.

Phylogeny & genetic diversity: The mitochondrial and nuclear phylogenies do not agree on the position of *U. nanus* (Figs. 2, 4-5). It clusters with *U. crassus* s. str. in the nuclear phylogeny and with *U. carneus* in the mitochondrial phylogeny (Figs. 2, 4-5). Whereas the nuclear phylogeny indicates a closer relationship between the two widespread and northern species (i.e. *U. nanus* and *U. crassus* s. str.), which share a large overlap in distribution, the mitochondrial phylogeny suggests that gene flow between *U. nanus* and *U. carneus* occurred in the Pliocene (Figs. 4-5).

The phylogeographic structure of this species includes a high diversity of haplotypes in the Rhine, Danube, and Meuse rivers, suggesting that it originated somewhere in these basins. The geological history of these basins is interrelated and complex. Prior to the Pliocene, the waters upstream of the present Upper Rhine (including the upper Rhône) were tributaries of the Danube. Later, they shifted westward towards the Rhône, although it is possible that a connection to the Danube persisted. Since the Pleistocene the Rhine system has taken its present northward course, joining the Scheldt and Meuse basins in a large delta (Preusser, 2008). The species appears to have spread more recently into the English Channel, North Sea, and Baltic basins, such as the Seine, Elbe, Oder, and Vistula, where genetic diversity is very low (Fig. 14).

Distribution: *Unio nanus* is restricted to Europe, with a core distribution in the Saône sub-catchment of the Rhône, the Rhine, and the Danube basins. The range of the species extends from these basins to the English Channel, North Sea, and Baltic Sea basins, from the Seine in the west to the Vistula in the east (Figs. 1 and 14).

Diagnosis: *Unio nanus* is represented by a unique genetic lineage in both the nuclear and mitochondrial genomes (Figs. 2, 4-5). Shell contour cannot be used to distinguish *U. nanus* from other species (Fig. 6; Tables 2 and S4). According to Haas (1969), the shells of *U. crassus cytherea*, here synonymised with *U. nanus*, are generally more convex, with the umbo more anterior than in *U. crassus* s. str. However, shell convexity in this species has been shown to be determined by habitat (Zając et al., 2018), making this character unreliable for species diagnosis. The species overlaps geographically with *U. crassus* s. str. over most of its range and with *U. vicarius* in the middle and lower Danube sections (Fig. 1).

Conservation: Populations have declined significantly throughout its distribution, and *U. nanus* is now highly threatened throughout its range. Potential differences in ecology and habitat requirements with *U. crassus* s. str. and the effects of hybridisation with *U. crassus* s. str. on the fitness, ecology, and behaviour of *U. nanus* should be investigated. As this species distribution overlaps extensively with *U. crassus* s. str. *and U. vicarius*, live specimens of *U. nanus* to be used for future potential conservation actions such as propagation and/or translocation should be subjected to molecular testing to ensure accurate species identification.

Unio sesirmensis Kobelt, 1913

Taxonomy: This species was described by Kobelt in 1913 based on specimens from the Bourguignat collection that had been sampled in Lake Suğla, which is connected to Lake Beyşehir. Kobelt placed it in the *pictorum* group, and concordantly Haas (1969) included it in the synonymy of *U. elongatulus eucirrus*. More recently, however, its status has been revised and *U.*

sesirmensis has been accepted as a valid species within the *U. crassus* complex (Lopes-Lima et al., 2021).

Phylogeny & genetic diversity: This species diverged early from the other species in the *U. crassus* complex. *U. sesirmensis* clusters with its southern neighbour *U. damascensis* in the nuclear phylogeny, whereas it represents an even more deeply divergent lineage in the mtDNA phylogenies (Figs. 2, 4-5). *Unio sesirmensis* shows some spatial genetic structure, with unique haplotypes for each of the Beyşehir and Tuz basins where it was found, although the region requires more extensive sampling to better understand its phylogeographic patterns. The phylogeographic patterns of this species have been described in detail by Lopes-Lima et al. (2021) and are therefore not depicted here.

Distribution: *Unio sesirmensis* occurs exclusively in streams of the Beyşehir and Tuz endorheic basins and probably in other freshwater habitats of the Central Anatolian Plateau in Türkiye (Fig. 1).

Diagnosis: The species represents a unique divergent genetic lineage in both the mitochondrial and nuclear genomes (Figs. 2-4). Morphometric analyses show that the shell contour is similar to *U. damascensis* and *U. desectus*, but different from other species (Tables 2 and S4). It has an exclusive distribution in the endorheic basins of Central Anatolia in Türkiye.

Conservation: Very little is known about the conservation status of this species, but wetlands in the Central Anatolian Plateau have been significantly reduced due to increasing water demands for agriculture. Dams, eutrophication, and water regulation are other known threats to streams and rivers where *U. sesirmensis* is known to occur. It is therefore highly likely that this species has declined significantly in recent decades due to habitat loss and degradation.

Unio tumidiformis da Silva e Castro, 1885

Taxonomy: It was described by da Silva e Castro in 1885 from specimens collected in the Sado River but was considered a junior synonym of *U. crassus* by Haas (1969) under the subspecies *Unio crassus batavus*. Its status was later revised using morphological and molecular data, and *U. tumidiformis* was re-established as a valid species from the *U. crassus* synonymy (Reis and Araujo, 2009).

Phylogeny & genetic diversity: The nuclear and mitochondrial phylogenies of this species are congruent and place *U. tumidiformis* basal to all other species in the *U. crassus* complex (Figs. 2-4). This species shows some geographic structure with unique haplotypes in the Sado River basin, but the lack of more systematic sampling across its distribution does not allow us to fully understand its phylogeography.

Distribution: This species is an Iberian endemic, occurring only in the river basins of the southwestern Iberian Peninsula, both in Portugal and Spain (Figs. 1 and 15). It is now restricted to the Mira, Sado, and Guadiana River basins, but was also originally present in the Guadalquivir, Mondego, and Tagus River basins (Reis and Araujo, 2009).

Diagnosis: Morphometric analyses revealed that *U. tumidiformis* has a rather distinctive shell contour (Tables 2 and S4). Other morphological characters, such as the strongly wavy umbonal rugae, a supra-cardinal tooth on the right valve and the lower height of the glochidium, have also been shown to be unique among species within the *U. crassus* complex (Araujo and Reis, 2009). The species shows a highly disjunct distribution compared to other species of the *U. crassus* complex (Figs. 1 and 15).

Conservation: The species is in sharp decline, practically extinct in the Sado River basin and with a very limited population in the Mira River basin. The species has also declined significantly in the Guadiana basin and is now threatened with extinction in many of its sub-basins. A recent extensive survey in Portugal revealed a sharp decline of 82% in population numbers and 48% in abundance over the last 20 years due to habitat loss and degradation (Lopes-Lima et al., 2023).

Unio vicarius Westerlund in Westerlund & Blanc, 1879 **stat. rev.**

Taxonomy: Described by Westerlund in 1879 from specimens collected in the River Sperchios in Sterea Ellada, central Greece, it was then placed by Haas (1969) in the synonymy of *U. crassus* under the subspecies *U. crassus bruguierianus*. Later, Araujo et al. (2018) revived the taxon *U. bruguierianus* using mitochondrial data but did not include the specimens collected from the Sperchios, Sofaditikos, and Aliakmon Rivers in this species, placing them under *Unio crassus*. More recently, *U. bruguierianus* has again been restricted to populations in northwestern Anatolia (Lopes-Lima et al., 2021). In this late study, the specimens collected by Araujo et al. (2018) from the Sperchios, Sofaditikos, and Aliakmon rivers were provisionally placed under *U. bruguierianus* due to low divergence in COI with the populations of *U. bruguierianus* from northwestern Anatolia (Lopes-Lima et al., 2021). Considering molecular and geographical arguments (see diagnosis below), *U. vicarius* is re-established here as a valid species from the synonymy of *U. bruguierianus*.

Phylogeny & genetic diversity: *Unio vicarius* is sister to *U. desectus* in the AHE phylogenies, whereas it is sister to *U. carneus* + *U. nanus* in the mitogenome phylogenies, and occupies a more basal position in the COI phylogeny as sister to *U. bruguierianus* + *U. mardinensis* (Figs. 2-5). The species shows high COI diversity and an interesting spatial genetic structure with unique haplotypes in the Sperchios and the Strymonas river basins (Fig. 16; Table 3). The configuration of the haplotype network and the high haplotype diversity in eastern Greece suggest that the species may have originated in this region and then expanded into the middle Danube, where the number of haplotypes is lower. This expansion may have occurred via a headwater river capture between the Aliakmon and the Danube, due to the proximity of headwater tributaries of both basins, which could explain the shared haplotype (haplotype 2: Fig. 16).

Distribution: The species has been reported from the upper reaches of the Aliakmonas, Pinios, and Struma/Strymonas river basins in Greece, Bulgaria, and North Macedonia. It has also been reported from the middle and lower Danube basin in Croatia, Romania, and Bulgaria, and is expected to occur in rivers within the same basin in Slovenia, Hungary, Bosnia and Herzegovina, and Serbia (Figs. 1 and 16).

Diagnosis: The species represents unique mitochondrial and nuclear lineages (Figs. 2, 4-5). The shell outline of *U. vicarius* is highly variable, with a large overlap with other species in the *U. crassus* complex. As a result, specimens belonging to this species were rarely assigned to the correct species based on morphometric data (Tables 2 and S4). The species is mostly parapatric with *U. desectus*, which occupies the upper and lower parts of the Pinios and Aliakmon basins, respectively (Fig. 1). The species overlaps with *U. nanus* and *U. crassus* s. str. in an extended area of the middle and lower Danube basin (Fig. 1).

Conservation: *Unio vicarius* has suffered a severe decline due to habitat loss and degradation throughout its range. Populations in the upper Aliakmonas, Pinios (Sofaditikos River), Sperchios (currently known from a single population), and Struma/Strymonas river basins have declined significantly, and the species is now very rare in Greece. There is no information on population trends in the middle and lower Danube, and considerable effort would be required in the future to obtain good quality information on this subject, as the species co-occurs with *U. crassus* s. str. and with *U. nanus*, from which it is morphologically very difficult to distinguish. Similarly, live

specimens of *U. vicarius* to be used for future potential conservation actions such as propagation and/or translocation should be subjected to molecular testing to ensure accurate species identification.

5. CONCLUSIONS

The current study, in a remarkable example of international scientific collaboration, successfully collected samples and molecular, distributional, and morphological data across a vast geographical range, covering most of Europe and parts of Asia, where populations of species belonging to the *U. crassus* complex were known to occur.

Using a combination of whole mitogenomes and nuclear markers derived from approximately 600 genes, we obtained data supporting the existence of 12 species within the *U. crassus* complex. Our results show that the evolutionary histories of the nuclear and mitochondrial genomes are not in complete agreement, although nuclear and mitogenomic topologies were often highly supported. These well-supported but inconsistent topologies reveal a rich evolutionary history for some of these species, with patterns of ancient hybridisation and/or polymorphism retention.

The taxonomic, distributional, and phylogeographic information gathered here has important implications for management and conservation, starting with the recognition of greater species diversity within the *U. crassus* complex than previously known, i.e. 12 species. All of these species are known or expected to be highly threatened and may benefit from being studied and managed independently. Key ecological and life-history traits are unknown for most of these species and should also be studied separately, particularly those related to habitat requirements and the reproductive cycle. Detailed species surveys are therefore urgently needed to determine the distribution, abundance, genetic diversity, and population structure of each species, as well as the range of host fish, microhabitats, behavioural traits (e.g. spurting behaviour; Aldridge et al., 2023b), growth, lifespan, and reproductive periods. Populations of species living in sympatry should be assessed for potential hybridisation and how such hybridisation may affect their fitness, in particular resilience to human disturbance, larval metamorphosis success, and the range of suitable host fish. Given the high congruence of the molecular results of the current study with the work of Haas (1969), where taxa were diagnosed on the basis of morphological characters, albeit without detailed explanation, a thorough study of anatomical and conchological characters is urgently needed to identify diagnostic morphological features that would allow the construction of an identification key for these species in the field.

Declaration of Competing Interest

The authors declare that they have no known competing financial interests or personal relationships that appear to have influenced the work reported in this paper.

Acknowledgements

We thank Ana-Maria Benedek, Monica Sîrbu and Jouni Leinikki for their assistance with the fieldwork, and to Jeroen Goud, Sankurie Pye, Fiona Ware, Emily Mitchell, and Aleksandra Skawina for their assistance with the taxonomic investigation. We would also like to thank the editor, Dr. Guillermo Ortí, and two anonymous reviewers for their time and effort in reviewing our manuscript and for their insightful comments and valuable improvements to our work. This publication is based upon work from COST Action CA18239: CONFREMU - Conservation of

freshwater mussels: a pan-European approach, supported by COST (European Cooperation in Science and Technology), including STSMs, the interaction of the authors and the writing of the paper. This work was supported by the project ConBiomics: The Missing Approach for the Conservation of Freshwater Bivalves Project No. NORTE-01-0145- FEDER-030286, co-financed by COMPETE 2020, Portugal 2020 and the European Union through the ERDF, and by FCT - Fundação para a Ciência e a Tecnologia, through national funds, strategic funding UIDB/04423/2020 and UIDP/04423/2020 provided by FCT. FCT also supported DVG (2020.03848.CEECIND) and MLL (2020.03608.CEECIND). INB, AVK and IVV were supported by the Russian Science Foundation under grants (19-14-00066-P), (21-17-00126) and (21-74-10130) respectively. BVB acknowledges the bioinformatics platform of UMR 8198 for the computing resources to perform time-calibrated phylogenetic analyses; this platform is in part funded by CPER research project CLIMIBIO through the French Ministère de l'Enseignement Supérieur et de la Recherche, the Agence Nationale de la Recherche, the European Fund for Regional Development (FEDER) and the region Hauts-de-France (HdF). Support to KD came from the Czech Science Foundation (19–05510S). TT and MT were supported by the National Science Fund of Bulgaria under the project 'Conservation of freshwater mussels on the Balkan Peninsula' (KP-06-COST-9/20.07.2022). Any use of trade, firm, or product names is for descriptive purposes only and does not imply endorsement by the United States Government.

References

Aldridge, D. C., Ollard, I. S., Bespalaya, Y. V., Bolotov, I. N., Douda, K., Geist, J., Haag, W. R., Klunzinger, M. W., Lopes-Lima, M., Mlambo, M. C. and Riccardi, N., 2023a. Freshwater mussel conservation: A global horizon scan of emerging threats and opportunities. Glob. Chang. Biol. 29, 575–589. https://doi.org/10.1111/gcb.16510

Aldridge, D. C., Brian J. I., Ćmiel, A., Lipińska, A., Lopes-Lima, M., Sousa, R., Teixeira, A., Zając, K., Zając, T., 2023b. Fishing for hosts: Larval spurting by the endangered thick-shelled river mussel, *Unio crassus*. Ecology 104, e4026. https://doi.org/10.1002/ecy.4026

Araujo, R., Gómez, I., Machordom, A., 2005. The identity and biology of *Unio mancus* Lamarck, 1819 (=*U. elongatulus*) (Bivalvia: Unionidae) in the Iberian Peninsula. J. Molluscan Stud. 71, 25–31. https://doi.org/10.1093/mollus/eyi002

Araujo, R., Toledo, C., Machordom, A., 2009. Redescription of *Unio gibbus* Spengler, 1793, A West Palaearctic freshwater mussel with hookless glochidia. Malacologia 51, 131–141. https://doi.org/10.4002/040.051.0109

Araujo, R., Buckley, D., Nagel, K.-O., Machordom, A., 2017. *Potomida littoralis* (Bivalvia, Unionidae) evolutionary history: slow evolution or recent speciation? Zool. J. Linn. Soc. 179, 277–290. https://doi.org/10.1111/zoj.12470

Araujo, R., Buckley, D., Nagel, K.-O., García-Jiménez, R., Machordom, A., 2018. Species boundaries, geographic distribution and evolutionary history of the Western Palaearctic

freshwater mussels *Unio* (Bivalvia: Unionidae). Zool. J. Linn. Soc. 182, 275–299. https://doi.org/10.1093/zoolinnean/zlx039

Babushkin, E.S., Vinarski, M.V., Kondakov, A.V., Tomilova, A.A., Grebennikov, M.E., Stolbov, V.A., Bolotov, I.N., 2021. European freshwater mussels (*Unio* spp., Unionidae) in Siberia and Kazakhstan: Pleistocene relicts or recent invaders? Limnologica 90, 125903. https://doi.org/10.1016/j.limno.2021.125903

Bolotov, I.N., Kondakov, A.V., Konopleva, E.S., Vikhrev, I.V., Aksenova, O.V., Aksenov, A.S., Bespalaya, Y.V., Borovskoy, A.V., Danilov, P.P., Dvoryankin, G.A., Gofarov, M.Y., Kabakov, M.B., Klishko, O.K., Kolosova, Y.S., Lyubas, A.A., Novoselov, A.P., Palatov, D.M., Savvinov, G.N., Solomonov, N.M., Spitsyn, V.M., Sokolova, S.E., Tomilova, A.A., Froufe, E., Bogan, A.E., Lopes-Lima, M., Makhrov, A.A., Vinarski, M.V., 2020. Integrative taxonomy, biogeography and conservation of freshwater mussels (Unionidae) in Russia. Sci. Rep. https://doi.org/10.1038/s41598-020-59867-7

Boore, J.L., 1999. Animal mitochondrial genomes. Nucleic Acids Res. 27, 1767–1780. https://doi.org/10.1093/nar/27.8.1767

Bouckaert, R., Vaughan, T.G., Barido-Sottani, J., Duchêne, S., Fourment, M., Gavryushkina, A., Heled, J., Jones, G., Kühnert, D., De Maio, N., Matschiner, M., Mendes, F.K., Müller, N.F., Ogilvie, H.A., du Plessis, L., Popinga, A., Rambaut, A., Rasmussen, D., Siveroni, I., Suchard, M.A., Wu, C.-H., Xie, D., Zhang, C., Stadler, T., Drummond, A.J., 2019. BEAST 2.5: An advanced software platform for Bayesian evolutionary analysis. PLOS Comput. Biol. 15, e1006650. https://doi.org/10.1371/journal.pcbi.1006650

Breinholt, J.W., Earl, C., Lemmon, A.R., Lemmon, E.M., Xiao, L., Kawahara, A.Y., 2018. Resolving Relationships among the Megadiverse Butterflies and Moths with a Novel Pipeline for Anchored Phylogenomics. Syst. Biol. 67, 78–93. https://doi.org/10.1093/sysbio/syx048

Breton, S., Stewart, D.T., Shepardson, S., Trdan, R.J., Bogan, A.E., Chapman, E.G., Ruminas, A.J., Piontkivska, H., Hoeh, W.R., 2011. Novel protein genes in animal mtDNA: a new sex determination system in freshwater mussels (Bivalvia: Unionoida)? Mol. Biol. Evol. 28, 1645–1659

Campbell, C. S., Dutoit, L., King, T. M., Craw, D., Burridge, C. P., Wallis, G. P., Waters, J. M., 2022. Genome-wide analysis resolves the radiation of New Zealand's freshwater *Galaxias vulgaris* complex and reveals a candidate species obscured by mitochondrial capture. Divers. Distrib. 28, 2255–2267. https://doi.org/10.1111/ddi.13629

Capella-Gutiérrez, S., Silla-Martínez, J.M., Gabaldón, T., 2009. trimAl: a tool for automated alignment trimming in large-scale phylogenetic analyses. Bioinformatics 25, 1972–1973. https://doi.org/10.1093/bioinformatics/btp348

Chen, J., 1987. Microstructures of Lower-Middle Jurassic unionid (Bivalvia) shells. Acta Palaeontol. Sin. 26, 8–17.

Chong, J.P., Harris, J.L., Roe, K.J., 2016. Incongruence between mtDNA and nuclear data in the freshwater mussel genus *Cyprogenia* (Bivalvia: Unionidae) and its impact on species delineation. Ecol. Evol. 6, 2439–2452. https://doi.org/10.1002/ece3.2071

Clement, M., Posada, D., Crandall, K.A., 2000. TCS: a computer program to estimate gene genealogies. Mol. Ecol. 9, 1657–1659. https://doi.org/10.1046/j.1365- 294x.2000.01020.x

Crampton, J.S., Haines, A.J., 1996. Users' manual for programs HANGLE, HMATCH and HCURVE for the Fourier shape analysis of two-dimensional outlines Ins. Geol. Nucl. Sci. Sci. Rep. 96.37, 1–28.

Dray, S., Dufour, A., 2007. The ade4 Package: Implementing the Duality Diagram for Ecologists. J. Stat. Soft., 22, 1–20. https://doi.org/10.18637/jss.v022.i04

EC, 2023. European Commission Life Public Database. < https://webgate.ec.europa.eu/life/publicWebsite/search > Accessed 10/9/2023.

Falkner, G., 1994. Systematik vorderorientalischer Najaden als Vorstudie zur Bearbeitung archäologischer Funde. Forschungen und Berichte zur Vor- und Frühgeschichte in Baden-Württemberg. In: Kokabi M, Wahl J (eds) Beiträge zur Archäozoologie und Prähistorischen Anthropolgie, vol 53. K Theiss, Stuttgart, pp 135–162.

Feind, S., Geist, J., Kuehn, R., 2018. Glacial perturbations shaped the genetic population structure of the endangered thick-shelled river mussel (*Unio crassus*, Philipsson 1788) in Central and Northern Europe. Hydrobiologia 810, 177–189. https://doi.org/10.1007/s10750-017-3134-2

Ferreira-Rodríguez, N., Akiyama, Y. B., Aksenova, O. V., Araujo, R., Barnhart, M. C., Bespalaya, Y. V., Bogan, A. E., Bolotov, I. N., Budha, P. B., Clavijo, C. and Clearwater, S. J., 2019. Research priorities for freshwater mussel conservation assessment. Biol. Conserv. 231, 77–87. https://doi.org/10.1016/j.biocon.2019.01.002

Froufe, E., Sobral, C., Teixeira, A., Sousa, R., Varandas, S., Aldridge, D. C., Lopes-Lima, M., 2014. Genetic diversity of the pan-European freshwater mussel *Anodonta anatina* (Bivalvia: Unionoida) based on CO1: new phylogenetic insights and implications for conservation. Aquat. Conserv. Mar. Freshw. Ecosyst. 24, 561–574. https://doi.org/10.1002/aqc.2456

Froufe, E., Gonçalves, D. V., Teixeira, A., Sousa, R., Varandas, S., Ghamizi, M., Zieritz, A., Lopes-Lima, M., 2016. Who lives where? Molecular and morphometric analyses clarify which *Unio* species (Unionida, Mollusca) inhabit the southwestern Palearctic. Org. Divers. Evol. 16, 597–611. https://doi.org/10.1007/s13127-016-0262-x

Froufe, E., Lopes-Lima, M., Riccardi, N., Zaccara, S., Vanetti, I., Lajtner, J., Teixeira, A., Varandas, S., Prié, V., Zieritz, A., Sousa, R., Bogan, A.E., 2017. Lifting the curtain on the freshwater mussel diversity of the Italian Peninsula and Croatian Adriatic coast. Biodivers. Conserv. 26, 3255–3274. https://doi.org/10.1007/s10531-017-1403-z

Froufe, E., Bolotov, I., Aldridge, D.C., Bogan, A.E., Breton, S., Gan, H.M., Kovitvadhi, U., Kovitvadhi, S., Riccardi, N., Secci-Petretto, G., Sousa, R., Teixeira, A., Varandas, S., Zanatta, D., Zieritz, A., Fonseca, M.M., Lopes-Lima, M., 2020. Mesozoic mitogenome rearrangements and freshwater mussel (Bivalvia: Unionoidea) macroevolution. Heredity 124, 182–196. https://doi.org/10.1038/s41437-019-0242-y

GBIF, 2023 GBIF Home Page. Available from: https://www.gbif.org [1 September 2022].

Geist, J., Kuehn, R., 2005. Genetic diversity and differentiation of central European freshwater pearl mussel (*Margaritifera margaritifera* L.) populations: Implications for conservation and management. Mol. Ecol. 14, 425–439. https://doi.org/10.1111/J.1365-294X.2004.02420.x

Geist, J., 2010. Strategies for the conservation of endangered freshwater pearl mussels (*Margaritifera margaritifera*): A synthesis of Conservation Genetics and Ecology. Hydrobiologia 644, 69–88. https://doi.org/10.1007/s10750-010-0190-2

Geist, J., 2011. Integrative freshwater ecology and biodiversity conservation. Ecol. Ind. 11: 1507-1516. https://doi.org/10.1016/j.ecolind.2011.04.002

Geist, J., Thielen, F., Lavictoire, L., Hoess, R., Altmueller, R., Baudrimont, M., Blaize, C., Campos, M., Carroll, P., Daill, D., Degelmann, W., Dettmer, R., Denic, M., Dury, P.,de Eyto, E., Grunicke, F., Gumpinger, C., Jakobsen, P.J., Kaldma, K., Klaas, K., Legeay, A., Mageroy, J.H., Moorkens, E.A., Motte, G., Nakamura, K., Ondina, P., Österling, M., Pichler-Scheder, M., Spisar,

O., Reis, J., Schneider, L.D., Schwarzer, A., Selheim, H., Soler, J., Taskinen, J., Taylor, J., Strachan, B., Wengström, N., Zając, T., in press. Captive breeding of European freshwater mussels as a conservation tool: a review. Aquat. Conserv. Mar. Freshw. Ecosyst.

Gomes-dos-Santos, A., Froufe, E., Pfeiffer, J., Johnson, N., Smith, C., Machado, A.M., Castro, L.F.C., Do, V.T., Hattori, A., Garrison, N., Whelan, N., Bolotov, I.N., Vikhrev, I.V., Kondakov, A.V., Ghamizi, M., Prié, V., Bogan, A.E., Lopes-Lima, M. (2023). A novel assembly pipeline and functional annotations for targeted sequencing: A case study on the globally threatened Margaritiferidae (Bivalvia: Unionida). Mol. Ecol. Res. 23: 1403-1422. https://doi.org/10.1111/1755-0998.13802

Gómez, A., Lunt, D.H., 2007. Refugia within refugia: patterns of phylogeographic concordance in the Iberian Peninsula. In: Weiss, S., Ferrand, N. (Eds.), Phylogeography of Southern European Refugia. Springer, Dordrecht, Netherlands, pp. 155–188. https://doi.org/10.1007/1-4020-4904-8_5

Graf, D.L., 2010. Funeral for the Nouvelle École -iana Generic Names Introduced for Freshwater Mussels (Mollusca: Bivalvia: Unionoida). Proc. Acad. Nat. Sci. Philadelphia 159, 1–23. https://doi.org/10.1635/053.159.0101

Graf, D.L., Cummings, K.S., 2023. The MUSSEL Project Database. < http://mussel-project.uwsp.edu/db/ > Accessed 10/9/2023.

Gu, Z.-W., 1998. Evolutionary trends in non-marine Cretaceous bivalves of Northeast China, in: Johnston, P.A., Haggart, J.W. (Eds.), Bivalves: An Eon of Evolution. University of Calgary Press, Calgary, pp. 267–276.

Haas, F., 1969. Superfamilia Unionacea. Das Tierreich, 88. Walter de Gruyter, Berlin.

Hammer, Ø., Harper, D.A.T., 2013. PAST version 3.22. Available at https://www.nhm.uio.no/english/research/infrastructure/past/

Henderson, J., 1935. Fossil non-marine Mollusca of North America. Geol. Soc. Am., Spec. Pap. 3, 1–313.

Hewitt, G.M. 1999. Post-glacial re-colonization of European biota. Biol. J. Linn. Soc. 68, 87–112. https://doi.org/10.1111/j.1095-8312.1999.tb01160.x

IUCN, 2023 The IUCN Red List of Threatened Species. Version 2023-1. https://www.iucnredlist.org. Accessed on [1 September 2023].

Japoshvili, B., Couto, T.B., Mumladze, L., Epitashvili, G., McClain, M.E., Jenkins, C. N., Anderson, E.P. 2021. Hydropower development in the Republic of Georgia and implications for freshwater biodiversity conservation. Biol. Conserv. 263, 109359. https://doi.org/10.1016/j.biocon.2021.109359

Johnston, P.A., Hendy, A.J.W., 2005. Paleoecology of mollusks from the Upper Cretaceous Belly River Group, in: Currie, P.J., Koppelhus, E.B. (Eds.), Dinosaur Provincial Park: A Spectacular Ancient Ecosystem Revealed. Indiana University Press, Bloomington, pp. 139–166.

Jombart, T., 2008. adegenet: a R package for the multivariate analysis of genetic markers. Bioinformatics, 24(11), 1403-1405. https://doi.org/10.1093/bioinformatics/btn129

Kalyaanamoorthy, S., Minh, B.Q., Wong, T.K.F., von Haeseler, A., Jermiin, L.S., 2017. ModelFinder: fast model selection for accurate phylogenetic estimates. Nat. Methods 14, 587–589. https://doi.org/10.1038/nmeth.4285

Katoh, K., Standley, D.M., 2013. MAFFT Multiple Sequence Alignment Software Version 7: Improvements in Performance and Usability. Mol. Biol. Evol. 30, 772–780. https://doi.org/10.1093/molbev/mst010

Kaya, M.Y., Dupont-Nivet, G., Proust, J.N., Roperch, P., Bougeois, L., Meijer, N., Frieling, J., Fioroni, C., Altıner, S.O., Vardar, E., Barbolini, N., Stoica, M., Aminov, J., Mamtimin, M., Guo, Z., 2019. Paleogene evolution and demise of the proto- Paratethys Sea in Central Asia (Tarim and Tajik basins): Role of intensified tectonic activity at ca. 41 Ma. Basin Res. 31, 461–486. https://doi.org/10.1111/bre.12330

Kaya, M.Y., Dupont-Nivet, G., Proust, J.N., Roperch, P., Meijer, N., Frieling, J., Fioroni, C., Altiner, S.O., Stoica, M., Aminov, J., Mamtimin, M., Guo, Z., 2020. Cretaceous evolution of the Central Asian proto-Paratethys Sea: Tectonic, eustatic, and climatic controls. Tectonics 39, e2019TC005983. https://doi.org/10.1029/2019TC005983

Khalloufi, N., Toledo, C., Machordom, A., Boumaiza, M., Araujo, R., 2011. The unionids of Tunisia: taxonomy and phylogenetic relationships, with redescription of *Unio ravoisieri* Deshayes, 1847 and *U. durieui* Deshayes, 1847. J. Molluscan Stud. 77, 103–115. https://doi.org/10.1093/mollus/eyq046

Kilikowska, A., Mioduchowska, M., Wysocka, A., Kaczmarczyk-Ziemba, A., Rychlińska, J., Zając, K., Zając, T., Ivinskis, P., Sell, J., 2020. The patterns and puzzles of genetic diversity of endangered freshwater mussel *Unio crassus* Philipsson, 1788 populations from Vistula and Neman drainages (Eastern Central Europe). Life 10, 119. https://doi.org/10.3390/life10070119

Klishko, O., Lopes-Lima, M., Froufe, E., Bogan, A., Vasiliev, L., Yanovich, L., 2017. Taxonomic reassessment of the freshwater mussel genus *Unio* (Bivalvia: Unionidae) in Russia and Ukraine based on morphological and molecular data. Zootaxa 4286, 93–112. https://doi.org/10.11646/zootaxa.4286.1.4

Klishko, O.K., Lopes-Lima, M., Froufe, E., Bogan, A.E., 2019. Solution of taxonomic status of *Unio mongolicus* Middendorff, 1851 (Bivalvia: Unionidae) from the type locality in Transbaikalia and history of its taxonomy. Ruthenica 29, 55–70.

Kotlik, P., Bogutskaya, N.G., Ekmekci, F.G., 2004. Circum Black Sea phylogeography of Barbus freshwater fishes: divergence in the Pontic glacial refugium. Mol. Ecol. 13, 87–95. https://doi.org/10.1016/j.ympev.2011.11.004

Kück, P., Longo, G.C., 2014. FASconCAT-G: extensive functions for multiple sequence alignment preparations concerning phylogenetic studies. Front. Zool. 11, 81. https://doi.org/10.1186/s12983-014-0081-x

Kumar, S., Stecher, G., Li, M., Knyaz, C., Tamura, K., 2018. MEGA X: Molecular evolutionary genetics analysis across computing platforms. Mol. Biol. Evol. 35, 1547–1549. https://doi.org/10.1093/molbev/msy096

Lanfear, R., Frandsen, P.B., Wright, A.M., Senfeld, T., Calcott, B., 2016. PartitionFinder 2: New methods for selecting partitioned models of evolution for molecular and morphological phylogenetic analyses. Mol. Biol. Evol. 34, 772–773. https://doi.org/10.1093/molbev/msw260

Lang, N., Wolff, E.W., 2011. Interglacial and glacial variability from the last 800 ka in marine, ice and terrestrial archives. Clim. Past 7, 361–380. https://doi.org/10.5194/cp-7-361-2011

Lehner, B., Grill, G., 2013. Global river hydrography and network routing: baseline data and new approaches to study the world's large river systems. Hydrol. Process. 27, 2171–2186. https://doi.org/10.1002/hyp.9740

Lopes-Lima, M., Teixeira, A., Froufe, E., Lopes, A., Varandas, S., Sousa, R., 2014. Biology and conservation of freshwater bivalves: past, present and future perspectives. Hydrobiologia 735, 1–13. https://doi.org/10.1007/s10750-014-1902-9

Lopes-Lima, M., Sousa, R., Teixeira, A., Varandas, S., Riccardi, N., Aldridge, D.C., Froufe, E., 2016. Newly developed microsatellite markers for the pan-European duck mussel, *Anodonta anatina*: revisiting the main mitochondrial lineages. Aquat. Conserv. Mar. Freshw. Ecosyst. 26, 307–318. https://doi.org/10.1002/aqc.2575

Lopes-Lima, M., Froufe, E., Do, V.T., Ghamizi, M., Mock, K.E., Kebapçı, Ü., Klishko, O., Kovitvadhi, S., Kovitvadhi, U., Paulo, O.S., Pfeiffer III, J.M., Raley, M., Riccardi, N., Şereflişan, H., Sousa, R., Teixeira, A., Varandas, S., Wu, X., Zanatta, D.T., Zieritz, A., Bogan, A.E., 2017a. Phylogeny of the most species-rich freshwater bivalve family (Bivalvia: Unionida: Unionidae): Defining modern subfamilies and tribes. Mol. Phylogenet. Evol. 106, 174–191. https://doi.org/10.1016/j.ympev.2016.08.021

Lopes-Lima, M., Sousa, R., Geist, J., Aldridge, D.C., Araujo, R., Bergengren, J., Bespalaya, Y., Bódis, E., Burlakova, L., Van Damme, D., Douda, K., Froufe, E., Georgiev, D., Gumpinger, C., Karatayev, A., Kebapçı, Ü., Killeen, I., Lajtner, J., Larsen, B.M., Lauceri, R., Legakis, A., Lois, S., Lundberg, S., Moorkens, E., Motte, G., Nagel, K.O., Ondina, P., Outeiro, A., Paunovic, M., Prié, V., von Proschwitz, T., Riccardi, N., Rudzite, M., Rudzitis, M., Scheder, C., Seddon, M., Şereflişan, H., Simíc, V., Sokolova, S., Stoeckl, K., Taskinen, J., Teixeira, A., Thielen, F., Trichkova, T., Varandas, S., Vicentini, H., Zajac, K., Zajac, T., Zogaris, S., 2017b. Conservation status of freshwater mussels in Europe: state of the art and future challenges. Biol. Rev. 92, 572–607. https://doi.org/10.1111/brv.12244

Lopes-Lima, M., Fonseca, M.M., Aldridge, D.C., Bogan, A.E., Gan, H.M., Ghamizi, M., Sousa, R., Teixeira, A., Varandas, S., Zanatta, D., Zieritz, A., Froufe, E., 2017c. The first Margaritiferidae male (M-type) mitogenome: mitochondrial gene order as a potential character for determining higher-order phylogeny within Unionida (Bivalvia). J. Molluscan Stud. 83, 249–252. https://doi.org/10.1093/mollus/eyx009

Lopes-Lima, M., Burlakova, L.E., Karatayev, A.Y., Mehler, K., Seddon, M., Sousa, R., 2018a. Conservation of freshwater bivalves at the global scale: diversity, threats and research needs. Hydrobiologia 810, 1–14. https://doi.org/10.1007/s10750-017- 3486-7

Lopes-Lima, M., Hinzmann, M., Varandas, S., Froufe, E., Reis, J., Moreira, C., Araújo, S., Miranda, F., Gonçalves, D. V., Beja, P., Sousa, R., Teixeira, A., 2020. Setting the stage for new ecological indicator species: A holistic case study on the Iberian dolphin freshwater mussel *Unio delphinus* Spengler, 1793. Ecol. Indic. 111, 105987. https://doi.org/10.1016/j.ecolind.2019.105987

Lopes-Lima, M., Gürlek, M.E., Kebapçı, Ü., Şereflişan, H., Yanık, T., Mirzajani, A., Neubert, E., Prié, V., Teixeira, A., Gomes-dos-Santos, A., Barros-García, D., Bolotov, I.N., Kondakov, A. V., Vikhrev, I. V., Tomilova, A.A., Özcan, T., Altun, A., Gonçalves, D. V., Bogan, A.E., Froufe, E., 2021. Diversity, biogeography, evolutionary relationships, and conservation of Eastern Mediterranean freshwater mussels (Bivalvia: Unionidae). Mol. Phylogenet. Evol. 163, 107261. https://doi.org/10.1016/j.ympev.2021.107261

Lopes-Lima, M., Reis, J., Alvarez, M.G., Anastácio, P.M., Banha, F., Beja, P., Castro, P., Gama, M., Gil, M.G., Gomes-dos-Santos, A., Miranda, F., Nogueira, J.G., Sousa, R., Teixeira, A., Varandas, S., Froufe, S., 2023. The silent extinction of freshwater mussels in Portugal. Biol. Conserv. 285, 110244. https://doi.org/10.1016/j.biocon.2023.110244

Lyubas, A.A., Kondakov, A. V., Tomilova, A.A., Gofarov, M.Y., Eliseeva, T.A., Konopleva, E.S., Vikhrev, I. V., Yunitsyna, O.A., Pešić, V., Bolotov, I.N., 2022. Taxonomic Reassessment of Freshwater Mussels from the Western Balkans Reveals an Overlooked but Critical Refugium and Defines Conservation Priorities. Diversity 14, 935. https://doi.org/10.3390/d14110935

Mammola, S., Riccardi, N., Prié, V., Correia, R., Cardoso, P., Lopes-Lima, M., Sousa, R., 2020. Towards a taxonomically unbiased European Union biodiversity strategy for 2030. Proc. R. Soc. B Biol. Sci. 287, 20202166. https://doi.org/10.1098/rspb.2020.2166

Minh, B.Q., Schmidt, H.A., Chernomor, O., Schrempf, D., Woodhams, M.D., von Haeseler, A., Lanfear, R., 2020. IQ-TREE 2: New Models and Efficient Methods for Phylogenetic Inference in the Genomic Era. Mol. Biol. Evol. 37, 1530–1534. https://doi.org/10.1093/molbev/msaa015

Mioduchowska, M., Kaczmarczyk, A., Zając, K., Zając, T., Sell, J., 2016. Gender-Associated Mitochondrial DNA Heteroplasmy in Somatic Tissues of the Endangered Freshwater Mussel *Unio crassus* (Bivalvia: Unionidae): Implications for Sex Identification and Phylogeographical Studies. J. Exp. Zool. Part A Ecol. Genet. Physiol. 325, 610–625. https://doi.org/10.1002/jez.2055

MolluscaBase, 2023. MolluscaBase. < https://www.molluscabase.org/ > Accessed 10.09.2023.

Nagel, K.-O., 2000. Testing hypotheses on the dispersal and evolutionary history of freshwater mussels (Mollusca: Bivalvia: Unionidae). J. Evol. Biol. 13, 854–865. https://doi.org/10.1046/j.1420-9101.2000.00217.x

Naimo, T.J., Damschen, E.D., Rada, R.G., Monroe, E.M., 1998. Nonlethal evaluation of the physiological health of unionid mussels: methods for biopsy and glycogen analysis. J. North Am. Benthol. Soc. 17, 121–128. https://doi.org/10.2307/201468056

Neemuchwala, S., Johnson, N.A., Pfeiffer, J.M., Lopes-Lima, M., Gomes-dos-Santos, A., Froufe, E., Hillis, D.M., Smith, C.H., 2023. Coevolution With Host Fishes Shapes Parasitic Life Histories in a Group of Freshwater Mussels (Unionidae: Quadrulini). Bull. Soc. Syst. Biol. 2, 1–25. https://doi.org/10.18061/bssb.v2i1.8998

Perdices, A., Bohlen, J., Doadrio, I., 2008. The molecular diversity of Adriatic spined loaches (Teleostei, Cobitidae). Mol. Phylogenet. Evol. 46, 382–390. https://doi.org/10.1016/j.ympev.2007.05.007

Pfeiffer, J.M., Breinholt, J.W., Page, L.M., 2019. Unioverse: A phylogenomic resource for reconstructing the evolution of freshwater mussels (Bivalvia, Unionoida). Mol. Phylogenet. Evol. 137, 114–126. https://doi.org/10.1016/j.ympev.2019.02.016

Pfeiffer, J. M., Graf, D. L., Cummings, K. S., & Page, L. M., 2021. Taxonomic revision of a radiation of South-east Asian freshwater mussels (Unionidae: Gonideinae: Contradentini+Rectidentini). Invertebr. Syst. 35, 394–470. https://doi.org/10.1071/IS20044

Preusser, F., 2008. Characterisation and evolution of the River Rhine system. Neth. J. Geosci. 87, 7–19. https://doi.org/10.1017/S0016774600024008

Prié, V., Puillandre, N., Bouchet, P., 2012. Bad taxonomy can kill: molecular reevaluation of *Unio mancus* Lamarck, 1819 (Bivalvia : Unionidae) and its accepted subspecies. Knowl. Manag. Aquat. Ecosyst. 08. https://doi.org/10.1051/kmae/2012014

Prié, V., Puillandre, N., 2014. Molecular phylogeny, taxonomy, and distribution of French *Unio* species (Bivalvia, Unionidae). Hydrobiologia 735, 95–110. https://doi.org/10.1007/s10750-013-1571-0

Puillandre, N., Brouillet, S., Achaz, G., 2021. ASAP: assemble species by automatic partitioning. Mol. Ecol. Resour. 21, 609–620. https://doi.org/10.1111/1755-0998.13281

Rambaut, A., Drummond, A.J., Xie, D., Baele, G., Suchard, M.A., Susko, E., 2018. Posterior summarization in Bayesian phylogenetics using Tracer 1.7. Syst. Biol. 67, 901–904. https://doi.org/10.1093/sysbio/syy032

Rasband, W., 2008. ImageJ. Image processing and analysis in Java. Available at https://imagej.nih.gov/ij/index.html

Ratnasingham, S., Hebert, P.D.N., 2013. A DNA-based registry for all animal species: The Barcode Index Number (BIN) system. e66213. PLoS ONE 8. https://doi.org/2010.1371/journal.pone.0066213

Reis, J., Araujo, R., 2009. Redescription of *Unio tumidiformis* Castro, 1885 (Bivalvia, Unionidae), an endemism from the south-western Iberian Peninsula. J. Nat. Hist. 43, 1929–1945. https://doi.org/10.1080/00222930902993724

Riboulot, V., Ker, S., Sultan, N., Thomas, Y., Marsset, B., Scalabrin, C., Ruffine, L., Boulart, C., Ion, G., 2018. Freshwater lake to salt-water sea causing widespread hydrate dissociation in the Black Sea. Nat. Commun. 9, 117. https://doi.org/10.1038/s41467-017-02271-z

Riccardi, N., Froufe, E., Bogan, A.E., Zieritz, A., Teixeira, A., Vanetti, I., Varandas, S., Zaccara, S., Nagel, K.-O., Lopes-Lima, M., 2020. Phylogeny of European Anodontini (Bivalvia: Unionidae) with a redescription of *Anodonta exulcerata*. Zool. J. Linn. Soc. 189, 745–761. https://doi.org/10.1093/zoolinnean/zlz136

Ronquist, F., Teslenko, M., van der Mark, P., Ayres, D.L., Darling, A., Höhna, S., Larget, B., Liu, L., Suchard, M.A., Huelsenbeck, J.P., 2012. MrBayes 3.2: Efficient Bayesian Phylogenetic Inference and Model Choice Across a Large Model Space. Syst. Biol. 61, 539–542. https://doi.org/10.1093/sysbio/sys029

Ryan, W.B.F., Major, C.O., Lericolais, G., Goldstein, S.L., 2003. Catastrophic Flooding of the Black Sea. Annu. Rev. Earth Planet. Sci. 31, 525–554. https://doi.org/10.1146/annurev.earth.31.100901.141249

Sambrook, J., Fritsch, E.F., Maniatis, T., 1989. Molecular Cloning: A Laboratory Manual. Cold Harbor Spring Press, New York.

Sanderson, M.J., 2003. r8s: inferring absolute rates of molecular evolution and divergence times in the absence of a molecular clock. Bioinformatics 19, 301–302. https://doi.org/10.1093/bioinformatics/19.2.301

Sano, I., Saito, T., Ito, S., Ye, B., Uechi, T., Seo, T., Do, V.T., Kimura, K., Hirano, T., Yamazaki, D., Shirai, A., Kondo, T., Miura, O., Miyazaki, J.-I., Chiba, S., 2022. Resolving species-level

diversity of *Beringiana* and *Sinanodonta* mussels (Bivalvia: Unionidae) in the Japanese archipelago using genome-wide data. Mol. Phylogenet. Evol. 175, 107563. https://doi.org/10.1016/j.ympev.2022.107563

Schmitt, L., Morris, D., Kondolf, G. M., Schmitt, L., Mathias Kondolf, G., Schmitt, L., Morris, D., 2018. Managing floods in large river basins in Europe: The Rhine River, in: Serra-Llobet, A., Kondolf, G., Schaefer, K., Nicholson, S. (Eds.), Managing Flood Risk: Innovative Approaches from Big Floodplain Rivers and Urban Streams. Palgrave Macmillan, Cham, pp. 75–89. https://doi.org/10.1007/978-3-319-71673-2_4

Schneider, S., Böhme, M., Prieto, J., 2013. Unionidae (Bivalvia; Palaeoheterodonta) from the Palaeogene of northern Vietnam: exploring the origins of the modern East Asian freshwater bivalve fauna. J. Syst. Palaeontol. 11, 337–357. https://doi.org/10.1080/14772019.2012.665085

Šedivá, A., Janko, K., Šlechtová, V., Kotlík, P., Simonović, P., Delic, A., Vassilev, M., 2008. Around or across the Carpathians: colonization model of the Danube basin inferred from genetic diversification of stone loach (*Barbatula barbatula*) populations. Mol. Ecol. 17, 1277–1292. https://doi.org/10.1111/j.1365-294X.2007.03656.x

Sela, I., Ashkenazy, H., Katoh, K., Pupko, T., 2015. GUIDANCE2: accurate detection of unreliable alignment regions accounting for the uncertainty of multiple parameters. W7–W14 Nucleic Acids Res. 43. https://doi.org/10.1093/nar/gkv318

Smith, C.H., Pfeiffer, J.M., Johnson, N.A., 2020. Comparative phylogenomics reveal complex evolution of life history strategies in a clade of bivalves with parasitic larvae (Bivalvia: Unionoida: Ambleminae). Cladistics 36, 505–520. https://doi.org/10.1111/cla.12423I

Struck, T.H., Feder, J.L., Bendiksby, M., Birkeland, S., Cerca, J., Gusarov, V.I., Kistenich, S., Larsson, K.H., Liow, L.H., Nowak, M.D.., Stedje, B., 2018. Finding evolutionary processes hidden in cryptic species. Trends Ecol. Evol. 33, 153–163. https://doi.org/10.1016/j.tree.2017.11.007

Sun, W., Liu, X., Wu, R., Wang, W., Wu, Y., Ouyang, S., Wu, X., 2019. Declining freshwater mussel diversity in the middle and lower reaches of the Xin River Basin: Threat and conservation. Ecol. Evol. 9, 14142–14153. https://doi.org/10.1002/ece3.5849

Teiga-Teixeira, J., Froufe, E., Gomes-dos-Santos, A., Bogan, A.E., Karatayev, A.Y., Burlakova, L.E., Aldridge, D.C., Bolotov, I.N., Vikhrev, I. V., Teixeira, A., Varandas, S., Zanatta, D.T., Lopes-Lima, M., 2020. Complete mitochondrial genomes of the freshwater mussels *Amblema plicata* (Say, 1817), *Pleurobema oviforme* (Conrad, 1834), and *Popenaias popeii* (Lea, 1857)

(Bivalvia: Unionidae: Ambleminae). Mitochondrial DNA Part B 5, 2959–2961. https://doi.org/10.1080/23802359.2020.1791008

Walker, J.M., Curole, J.P., Wade, D.E., Chapman, E.G., Bogan, A.E., Watters, G.T., Hoeh, W.R., 2006. Taxonomic distribution and phylogenetic utility of gender-associated mitochondrial genomes in the Unionoida (Bivalvia). Malacologia 48, 265–282.

Walker, J.M., Bogan, A.E., Bonfiglio, E.A., Campbell, D.C., Christian, A.D., Curole, J.P., Harris, J.L., Wojtecki, R.J., Hoeh, W.R., 2007. Primers for amplifying the hypervariable, male-transmitted COII-COI junction region in amblemine freshwater mussels (Bivalvia: Unionoidea: Ambleminae): primer note. Mol. Ecol. Notes 7, 489–491. https://doi.org/10.1111/j.1471-286.2006.01630.x

Walker, K. F., Jones, H. A., Klunzinger, M. W. 2014. Bivalves in a bottleneck: taxonomy, phylogeography and conservation of freshwater mussels (Bivalvia: Unionoida) in Australasia. Hydrobiologia *735*, 61–79. https://doi.org/10.1007/s10750-013-1522-9

Waters, J. M., Rowe, D. L., Burridge, C. P., Wallis, G. P. 2010. Gene trees versus species trees: reassessing life-history evolution in a freshwater fish radiation. Syst. Biol. 59, 504–517. https://doi.org/10.1093/sysbio/syq031

Weiss, S., Ferrand, N., 2006. Current perspectives in phylogeography and the significance of South European refugia in the creation and maintenance of European biodiversity, Chapter XIV. In: Weiss, S., Ferrand, N. (Eds.), Phylogeography of Southern European Refugia. Springer, The Netherlands, pp. 341–357. https://doi.org/10.1007/1-4020-4904-8_14

Zając, K., Zając, T., Ćmiel, A., 2018. What can we infer from the shell dimensions of the thick-shelled river mussel *Unio crassus*? Hydrobiologia 810, 415–431. https://doi.org/10.1007/s10750-017-3098-2

Zieritz, A., Hoffman, J.I., Amos, W., Aldridge, D.C., 2010. Phenotypic plasticity and genetic isolation-by-distance in the freshwater mussel *Unio pictorum* (Mollusca: Unionoida). Evol. Ecol. 24, 923–938. https://doi.org/10.1007/s10682-009-9350-0

Zogaris, S., Economou, A.N., 2017. The Biogeographic Characteristics of the River Basins of Greece, in: Skoulikidis, N., Dimitriou, E., Karaouzas, I. (Eds.), The Rivers of Greece. The Handbook of Environmental Chemistry, vol 59. Springer, Berlin, Heidelberg, pp. 53–95. https://doi.org/10.1007/698_2017_475

Zykin, V.S., 1979. Stratigraphy and the Pliocene unionids of the south of the West Siberian Plain [in Russian]. Nauka, Novosibirsk, 137 pp.

Zykin, V.S., 2012. Stratigraphy and evolution of the natural environment and climate in the late Cenozoic of the south of Western Siberia [in Russian]. Geo, Novosibirsk, 487 pp.

Further reading

Audibert, C., Breure, A.S.H., 2021. Joseph Henry Drouët (1827-1900): a biographical sketch, bibliography and his contributions to malacology. Arch. Molluskenkd 150, 87–106. https://doi.org/10.1127/arch.moll/150/087-106

Chen, J. 1983. Microstructure of Early and Middle Jurassic unionids. Trans. Chin. Soc. Malacol. 1, 221–222.

Gou, Z., Huang, B., Chen, C., Wen, S., Ma, Q., Lan, X., Xu, J., Liu, L., Wang, S., Wang, D., Qiu, R., Huang, Z., Zhang, Z., Chen, J., Wu, P., 1976. Chinese fossils of all groups. Fossil Lamellibranchia of China [in Chinese]. Nanjing, Beijing: Nanjing Institute of Geology and Palaeontology, Academia Sinica, Science Press.

Rossmässler, E.A., W. Kobelt, with parts by Oskar Boettger, Fritz Haas, Paul Hesse, Hermann Rolle, and Johann Andreas Wagner (1835-1920). Iconographie der Land- und Süsswasser-Mollusken, mit vorzüglicher Berücksichtigung der Europäischen noch nicht abgebildeten Arten. 30 vols.

Starobogatov, Y.I., Bogatov, V.V., Prozorova, L.A., Saenko, E.M., 2004. Molluscs [in Russian]. In S. J. Tsalolikhin (Ed.), Opredelitel' presnovodnykh bespozvonochnykh Rossii i sopredel'nykh territoriy (Vol. 6, pp. 6–491). Saint-Petersburg: Nauka.

Suzuki, K., 1949. Development of the fossil non-marine molluscan faunas in Eastern Asia. Jpn. J. Geol. Geogr. 21, 91–133.

Rossmässler, E. A. and W. Kobelt, with parts by Oskar Boettger, Fritz Haas, Paul Hesse, Hermann Rolle, and Johann Andreas Wagner (1835-1920). Iconographie der Land- und Süsswasser-Mollusken, mit vorzüglicher Berücksichtigung der Europäischen noch nicht abgebildeten Arten. 30 vols.

Captions to figures

Figure 1. Top: Distribution map of all *Unio crassus* subspecies depicted across the main river basins in shaded colours following Haas (1969), with coloured dots indicating the molecular lineages to which sampled populations belong. **Bottom**: Distribution map of all the species of the *U. crassus* complex recognized in the present study, depicted across the main river basins in shaded colours.

Figure 2. Bayesian Inference (BI) phylogenetic tree inferred from the *cytochrome c oxidase subunit I* (COI) gene fragment, and species delineation of the *Unio crassus* complex. Values above the branches are per cent posterior probabilities/ultrafast bootstrap supports. Vertical bars correspond to molecular operational taxonomic units according to different species delimitation methods: red - TCS (95%); green - BINS of BOLD; blue - ASAP; purple - bPTP; and black - consensus. Support values > 95% for both phylogenetic analyses are indicated by an asterisk, support values < 50% and those within each recognised MOTU have been deleted for clarity. Grey boxes around species names indicate species distinguishable only with AHE data.

Figure 3. LEFT: Principal Coordinates Analysis (PCoA) of the cytochrome c oxidase subunit I (COI) gene-fragment dataset including all sequences except those of *U. tumidiformis*. **RIGHT**: Map of the populations sequenced for COI with the PCoA colour coding; *U. tumidiformis* was added in white.

Figure 4. Bayesian Inference (BI) and Maximum likelihood (ML) phylogenetic trees of the *U. crassus* complex inferred from the whole mitogenomes (**Left**) and Anchored Hybrid Enrichment, AHE (**Right**) datasets. Support values > 95% for both phylogenetic analyses are indicated by an asterisk.

Figure 5. Time-calibrated phylogeny obtained using BEAST2 from alignments of the whole mitogenomes (**TOP**) and Anchored Hybrid Enrichment (**BOTTOM**) datasets and three fossil-based calibration points for the *U. crassus* complex.

Figure 6. Principal component (PC) scores of shell outlines for the first two PC axes obtained from 18 Fourier coefficients of all species within the *Unio crassus* complex. Synthetic shell outlines of 'extreme' morphotypes are shown with the anterior margin oriented towards the left and the dorsal margin towards the top of the page.

Figure 7. TOP: Distribution map of *Unio bruguierianus* in the study area, showing its potential distribution in the main river basins in orange and outlined in black. Coloured dots represent

sequenced populations. **BOTTOM**: COI haplotype (TCS) network showing the relationships of all new and previously published *U. bruguierianus* sequences (Table S1). Circle size is proportional to observed haplotype frequencies, each dash indicates a nucleotide substitution. Colours represent individuals from each basin.

Figure 8. LEFT: Distribution map of *Unio carneus* in the study area, showing its potential distribution in the main river basins in red and outlined in black. Coloured dots represent sequenced populations. **RIGHT**: COI haplotype (TCS) network showing the relationships of all new and previously published *Unio carneus* sequences (Table S1). Circle size is proportional to observed haplotype frequencies, each dash indicates a nucleotide substitution. Colours represent individuals from each basin.

Figure 9. TOP: Distribution map of *Unio crassus* s. str. in the study area, showing its potential distribution in the main river basins in purple and outlined in black. Coloured dots represent sequenced populations. **BOTTOM**: COI haplotype network (TCS) showing the relationships of all new and previously published *Unio crassus* s. str. sequences (Table S1). Circle size is proportional to observed haplotype frequencies, each dash indicates a nucleotide substitution. Colours represent individuals from each basin.

Figure 10. LEFT: Distribution map of *Unio desectus* in the study area, showing its potential distribution in the main river basins in blue and outlined in black. Coloured dots represent sequenced populations. **RIGHT**: COI haplotype network (TCS) showing the relationships of all new and previously published *Unio desectus* sequences (Table S1). Circle size is proportional to observed haplotype frequencies, each dash indicates a nucleotide substitution. Colours represent individuals from each basin.

Figure 11. TOP: Distribution map of *Unio gontierii* in the study area, showing its potential distribution in the main river basins in green and outlined in black. Coloured dots represent sequenced populations. **BOTTOM**: COI haplotype network (TCS) showing the relationships of all new and previously published *Unio gontierii* sequences (Table S1). Circle size is proportional to observed haplotype frequencies, each dash indicates a nucleotide substitution. Colours represent individuals from each basin.

Figure 12. LEFT: Distribution map of *Unio ionicus* in the study area, showing its potential distribution in the main river basins in red and outlined in black. Coloured dots represent sequenced populations. **RIGHT**: COI haplotype network (TCS) showing the relationships of all new and previously published *Unio ionicus* sequences (Table S1). Circle size is proportional to observed haplotype frequencies, each dash indicates a nucleotide substitution. Colours represent individuals from each basin.

Figure 13. LEFT: Distribution map of *Unio mardinensis* in the study area, showing its potential distribution in the main river basins in orange and outlined in black. Coloured dots represent sequenced populations. **RIGHT**: COI haplotype network (TCS) showing the relationships of all

new and previously published *Unio mardinensis* sequences (Table S1). Circle size is proportional to observed haplotype frequencies, each dash indicates a nucleotide substitution. Colours represent individuals from each basin.

Figure 14. TOP: Distribution map of *Unio nanus* in the study area, showing its potential distribution in the main river basins in blue and outlined in black. Coloured dots represent sequenced populations. **BOTTOM**: COI haplotype network (TCS) showing the relationships of all new and previously published *Unio nanus* sequences (Table S1). Circle size is proportional to observed haplotype frequencies, each dash indicates a nucleotide substitution. Colours represent individuals from each basin.

Figure 15. TOP: Distribution map of *Unio tumidiformis* in the study area, showing its potential distribution in the main river basins in green and outlined in black. Coloured dots represent sequenced populations. **BOTTOM**: COI haplotype network (TCS) showing the relationships of all new and previously published *Unio tumidiformis* sequences (Table S1). Circle size is proportional to observed haplotype frequencies, each dash indicates a nucleotide substitution. Colours represent individuals from each basin.

Figure 16. TOP: Distribution map of *Unio vicarius* in the study area, showing its potential distribution in the main river basins in yellow and outlined in black. Coloured dots represent sequenced populations. **BOTTOM**: COI haplotype network (TCS) showing the relationships of all new and previously published *Unio vicarius* sequences (Table S1). Circle size is proportional to observed haplotype frequencies, each dash indicates a nucleotide substitution. Colours represent individuals from each basin.

Figure S1. Bayesian Inference (BI) phylogenetic tree inferred from the cytochrome *c* oxidase subunit I (COI) gene fragment, and species delineation of the *Unio crassus* complex. Values above the branches are percent posterior probabilities/ultrafast bootstrap supports. Vertical bars correspond to molecular operational taxonomic units according to different species delimitation methods: red - TCS (95%); green - BINS of BOLD; blue - ASAP; purple - bPTP; and black - consensus. Support values > 95% for both phylogenetic analyses are indicated by an asterisk, support values < 50% and those within each recognised MOTU have been deleted for clarity. Grey boxes around species names indicate species distinguishable only with AHE data.

Figure S2. LEFT: Principal Coordinates Analysis (PCoA) of the cytochrome c oxidase subunit I (COI) gene-fragment dataset for the *U. crassus* complex including all sequences. **RIGHT**: Map of the populations sequenced for COI with the PCoA colour coding.

Figure S3. Bayesian Inference (BI) and Maximum likelihood (ML) phylogenetic tree for the *U. crassus* complex inferred from the flanking region only of the Anchored Hybrid Enrichment, AHE dataset. Support values > 95% for both phylogenetic analyses are indicated by an asterisk.

Figure S4. Bayesian Inference (BI) and Maximum likelihood (ML) phylogenetic tree for the *U. crassis* complex inferred from the target region only of the Anchored Hybrid Enrichment, AHE dataset. Support values > 95% for both phylogenetic analyses are indicated by an asterisk.

AUTHOR CONTRIBUTIONS:

Study conception and design MLL, JG, SE, EF

Draft manuscript preparation: MLL with text contributions by BVB, JG, AZ

Laboratory work (genetics): SE, BA, OAC, AGS, VF, AVK, RK

Molecular Analyses: MLL, BVB, NJ, AGS, JP, CHS, JV, EF

Fossil calibration: BVB

Morphometry: AZ

Taxonomy: MLL, AEB, K-ON, VP

Fieldwork: MLL, SE, JG, LB, AEB, AB, INB, OAC, KD, DVG, MEG, IK, AVK, JL, UK, RK, MÖ, VP, NR, LDS, IS, SG, SR, SS, JS, KS, JT, AT, MT, TT, LM, MU, SVäl, SVar, IVV, KZ, TZ, SZ

All authors contributed to the interpretation of the results and the final version of the manuscript.

Highlights

. Freshwater mussels of the *Unio crassus* complex were sampled comprehensively throughout Eurasia.

. Sequences of COI, whole mitogenomes and nuclear Anchored Hybrid Enrichment were used to infer phylogenies.

. The *Unio crassus* complex was divided into 12 geographically structured species.

. Morphometry of the shell outline revealed morphospace overlaps among several species.

. New systematics, taxonomy, and conservation remarks on these species are provided.

Table 1. List of species recognized within the *Unio crassus* complex in the present study, the cytochrome oxidase c subunit I (COI) gene fragment pairwise genetic distance (% uncorrected *p*-distance) matrixes among them (in black), and associated standard error (in blue). Mitochondrial introgression between species pairs (in red).

UNIONINAE Unionini Rafinesque, 1820 *Unio* (*crassus*-clade)	*U. bruguierianus*	*U. carneus*	*U. crassus*	*U. damascensis*	*U. desectus*	*U. gontierii*	*U. ionicus*	*U. mardinensis*	*U. nanus*	*U. sesirmensis*	*U. tumidiformis*	*U. vicarius*
U. bruguierianus Bourguignat, 1853		0.70	0.60	0.75	0.75	0.65	0.79	0.28	0.59	0.96	1.00	0.50
U. carneus Küster, 1854	4.02		0.68	0.82	0.83	0.72	0.83	0.72	0.65	1.04	1.15	0.62
U. crassus Philipsson in Retzius, 1788	3.08	3.62		0.65	0.71	0.31	0.89	0.62	0.62	0.93	1.11	0.61
U. damascensis Lea, 1863	4.07	4.97	3.34		0.75	0.71	0.87	0.79	0.76	0.86	1.05	0.78

U. desectus Westerlund, 1879	4.26	5.17	3.98	4.06		0.76	0.83	0.80	0.76	0.90	1.14	0.78
U. gontieri Bourguignat, 1856	3.24	3.83	1.08	3.58	4.29		0.90	0.68	0.65	0.95	1.07	0.65
U. ionicus Drouët, 1879	4.26	5.50	4.21	4.64	4.59	4.30		0.88	0.76	1.03	1.10	0.85
U. mardinensis Lea, 1865	1.31	3.38	2.90	4.26	4.41	3.14	4.55		0.59	1.05	1.09	0.51
U. nanus Lamarck, 1819	3.49	3.12	2.90	4.31	4.61	3.01	4.30	3.17		0.95	1.10	0.49
U. sesirmensis Kobelt, 1913	6.24	7.71	5.90	5.27	5.15	6.03	6.49	6.68	6.36		1.23	1.01
U. tumidiformis Castro, 1885	7.67	9.74	8.38	8.80	8.30	8.77	9.39	7.72	8.62	9.76		1.09
U. vicarius Westerl	2.37	3.21	2.31	3.74	4.08	2.40	4.20	2.08	2.54	6.29	8.44	

und, 1879	

Table 2. Adjusted P-values (<0.05 in bold) (a) obtained by Tukey's pairwise posthoc-tests following ANOVAs testing for significant differences between *Unio* species in PC1 (upper right) and PC2 (lower left) values, respectively, obtained by PCA on 18 Fourier coefficients obtained by Fourier Shape Analysis of shell outlines, and (b) ANOSIM of all 18 Fourier coefficients.

(a) PC2\PC1	*bruguierianus*	*carneus*	*crassus*	*damascensis*	*desectus*	*gontieri*	*ionicus*	*mardinensis*	*nanus*	*sesirmensis*	*tumidiformis*	*vicarius*
bruguierianus		**0.0010**	0.4284	**<0.0001**	0.9998	0.5451	0.9941	0.9859	0.4172	0.7968	1.0000	0.6892
carneus	**0.0005**		**0.0480**	0.6384	0.3645	0.9702	0.5075	**0.0010**	**0.0471**	0.9503	0.5491	0.1173
crassus	**0.0246**	**<0.0001**		**<0.0001**	1.0000	0.9919	1.0000	0.2902	1.000	0.9995	1.0000	1.0000
damascensis	0.9945	0.0950	**0.0226**		**0.00005**	**0.0385**	**0.00010**	**<0.0001**	**<0.0001**	**0.0411**	**0.0146**	**<0.0001**
desectus	**0.0350**	**<0.0001**	0.7578	**0.0103**		0.9958	1.0000	0.9379	1.0000	0.9994	1.0000	1.0000

gontierii	**0.0010**	**<0.0001**	0.1718	**0.0004**	1.0000		0.9995	0.2302	0.9919	1.0000	0.9926	0.9971
ionicus	0.9155	**0.0004**	1.0000	0.5919	0.9502	0.6122		0.8110	1.0000	1.0000	1.0000	1.0000
mardinensis	1.0000	0.0636	0.5065	1.0000	0.1018	**0.0100**	0.9304		0.2872	0.4148	0.9995	0.3648
nanus	0.3692	**<0.0001**	0.9656	0.1702	0.4054	**0.0406**	1.0000	0.8730		0.9995	1.0000	1.0000
sesirmensis	1.0000	**0.0127**	0.9959	0.9737	0.7089	0.2769	1.0000	0.9996	1.0000		0.9980	0.9998
tumidiformis	1.0000	0.3178	0.9974	1.0000	0.7241	0.3701	1.0000	1.0000	0.9999	1.0000		1.0000
vicarius	**0.0119**	**<0.0001**	0.9965	**0.0077**	0.9791	0.5925	1.0000	0.2487	0.6585	0.9830	0.9738	
(b) ANOSIM												
bruguierianus	**0.0066**	**0.0066**	**0.0066**	**0.0264**	1	1	**0.0066**	0.6864	**0.0330**	1	**0.0066**	
carneus		**0.0066**	**0.0066**	**0.0066**	**0.0066**	**0.0066**	**0.0066**	**0.0066**	**0.0264**	0.1848	**0.0066**	
crassus			**0.0066**	1	0.5742	1	**0.0066**	**0.0066**	1	1	1	

damascensis					**0.0066**	**0.0066**	**0.0066**	**0.0066**	**0.0066**	0.9570	0.1320	**0.0066**
desectus						**0.0066**	**0.0066**	0.0924	1	0.4488	**0.0264**	1
gontierii							**0.0198**	**0.0066**	1	**0.0066**	**0.0264**	1
ionicus								0.1386	1	**0.0066**	**0.0330**	1
mardinensis									**0.0066**	**0.0396**	1	**0.0264**
nanus										1	1	1
sesirmensis											**0.0264**	1
tumidiformis												1

Table 3. Number of COI-sequenced specimens, number of haplotypes (Haps), populations, independent river basins, haplotype (Hap.) diversity, nucleotide (Nuc.) diversity and average *p*-distance per species within the *Unio crassus*-species complex recognised in this study.

Species	Specimens	Haps	Populations	Basins	Hap. Diversity	Nuc. Diversity	*p*-distance
U. bruguierianus	76	21	17	11	0.896	0.01072	0.0107
U. carneus	29	9	6	1	0.768	0.00166	0.0017

U. crassus	241	31	56	27	0.784	0.00047	0.0033
U. damascensis	28	9	6	3	0.854	0.00643	0.0064
U. desectus	15	6	3	3	0.648	0.00223	0.0022
U. gontierii	30	10	10	6	0.844	0.00375	0.0038
U. ionicus	35	6	7	6	0.437	0.00079	0.0008
U. mardinensis	17	5	4	2	0.647	0.00231	0.0023
U. nanus	234	33	67	9	0.793	0.00594	0.0059
U. sesirmensis	10	5	2	1	0.822	0.00413	0.0041
U. tumidiformis	33	8	10	3	0.784	0.00455	0.0045
U. vicarius	67	13	15	6	0.825	0.00566	0.0057

Figure 1

Click here to access/download;Figure;Figure 1. Distributions + Haas + mtDNA R1.jpg

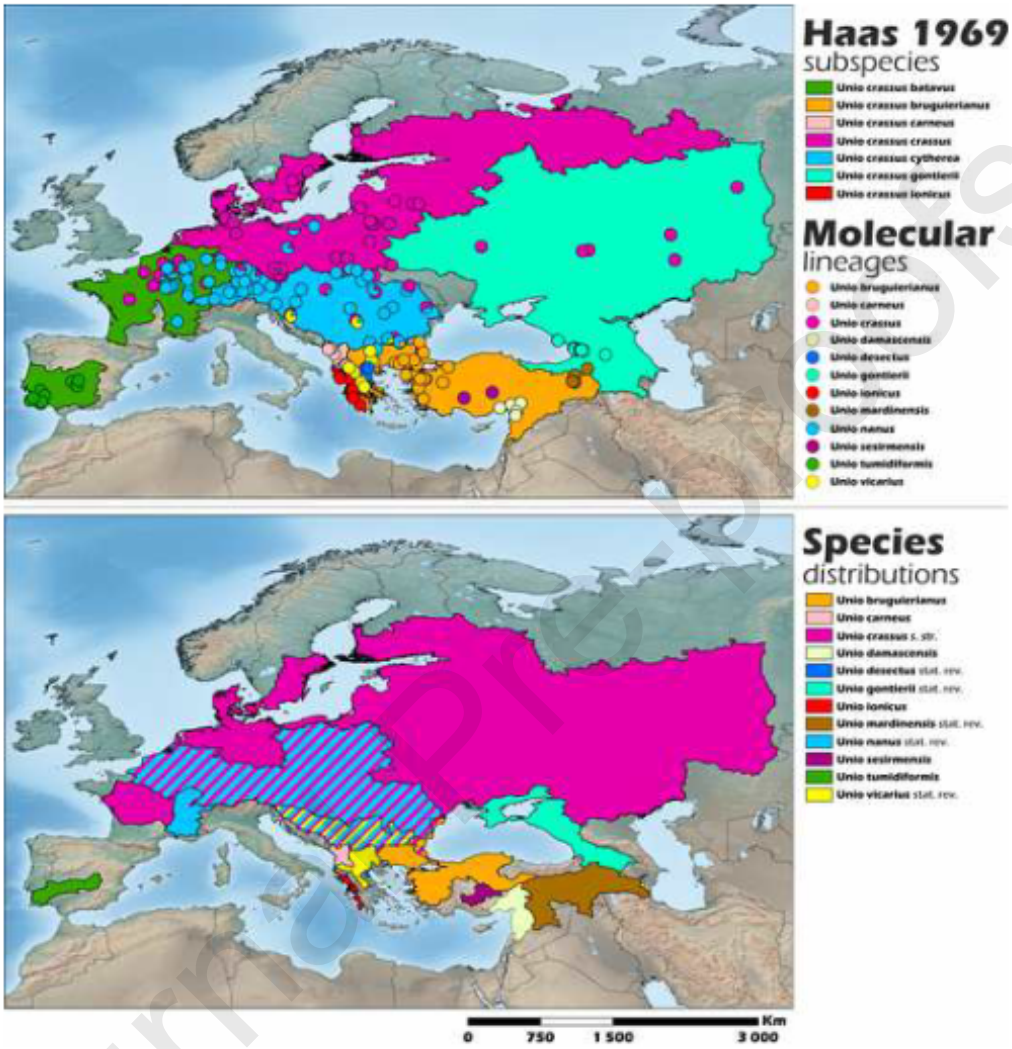

Figure 2

Click here to access/download;Figure;Figure 2. COI Tree collapsed + SDM R1.jpg

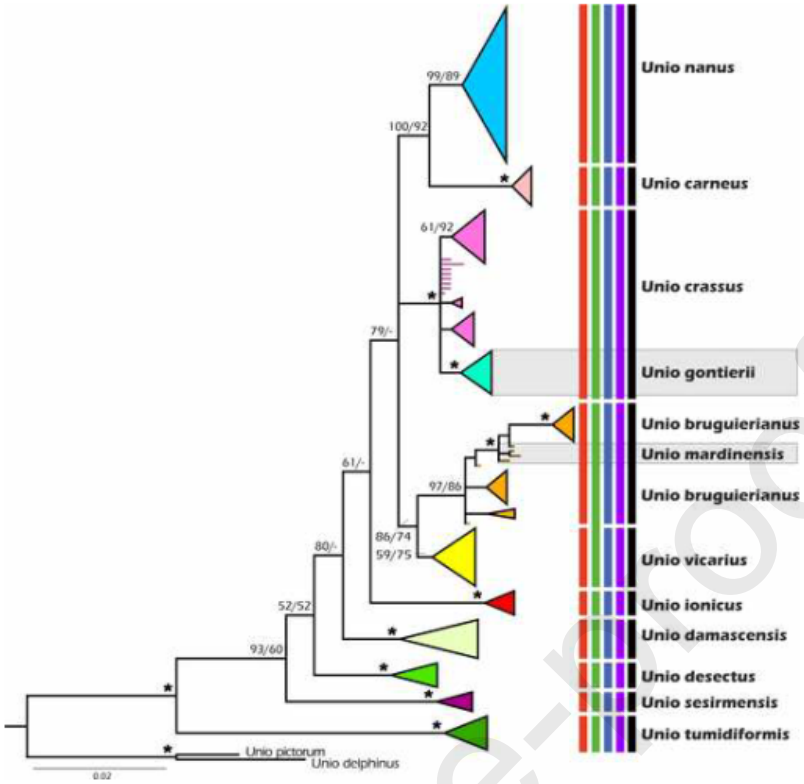

Figure 3

Click here to access/download;Figure;Figure 3. PCA No Tumidiformis.jpg

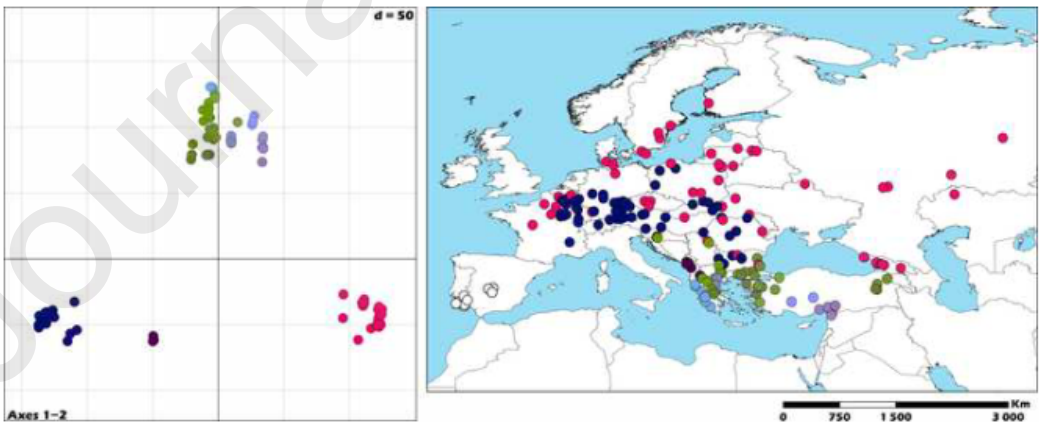

Figure 4

Click here to access/download;Figure;Figure 4. Mitogenomes + AHE Tree R1.jpg

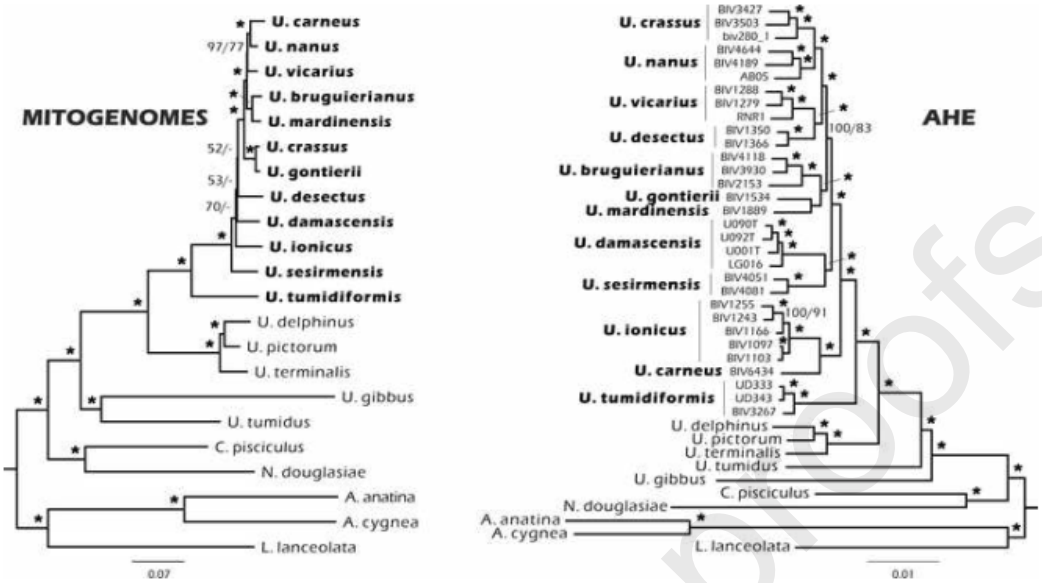

Figure 5

Click here to access/download;Figure;Figure 5. Time Mitogenomes + AHE Tree.jpg

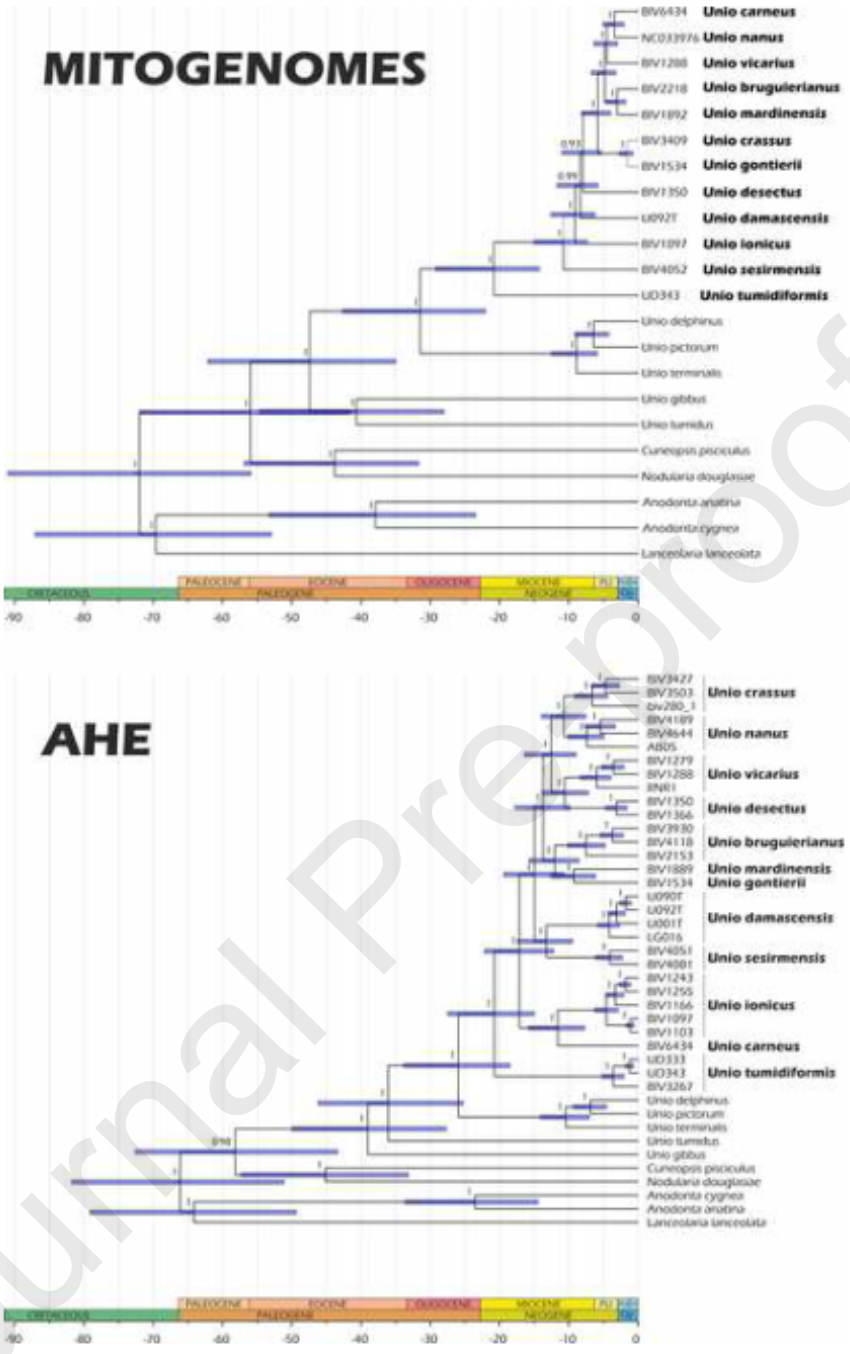

Figure 6

Click here to access/download;Figure;Figure 6. Morphometry Figure.jpg

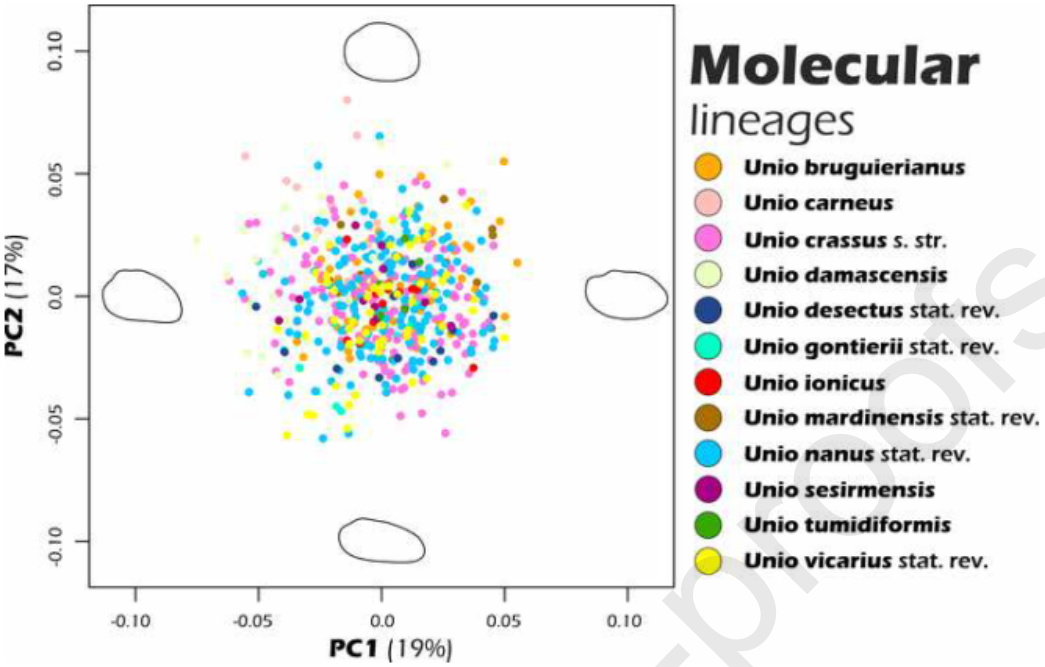

Figure 7

Click here to access/download;Figure;Figure 7. Hap Network + Map Bruguierianus.jpg

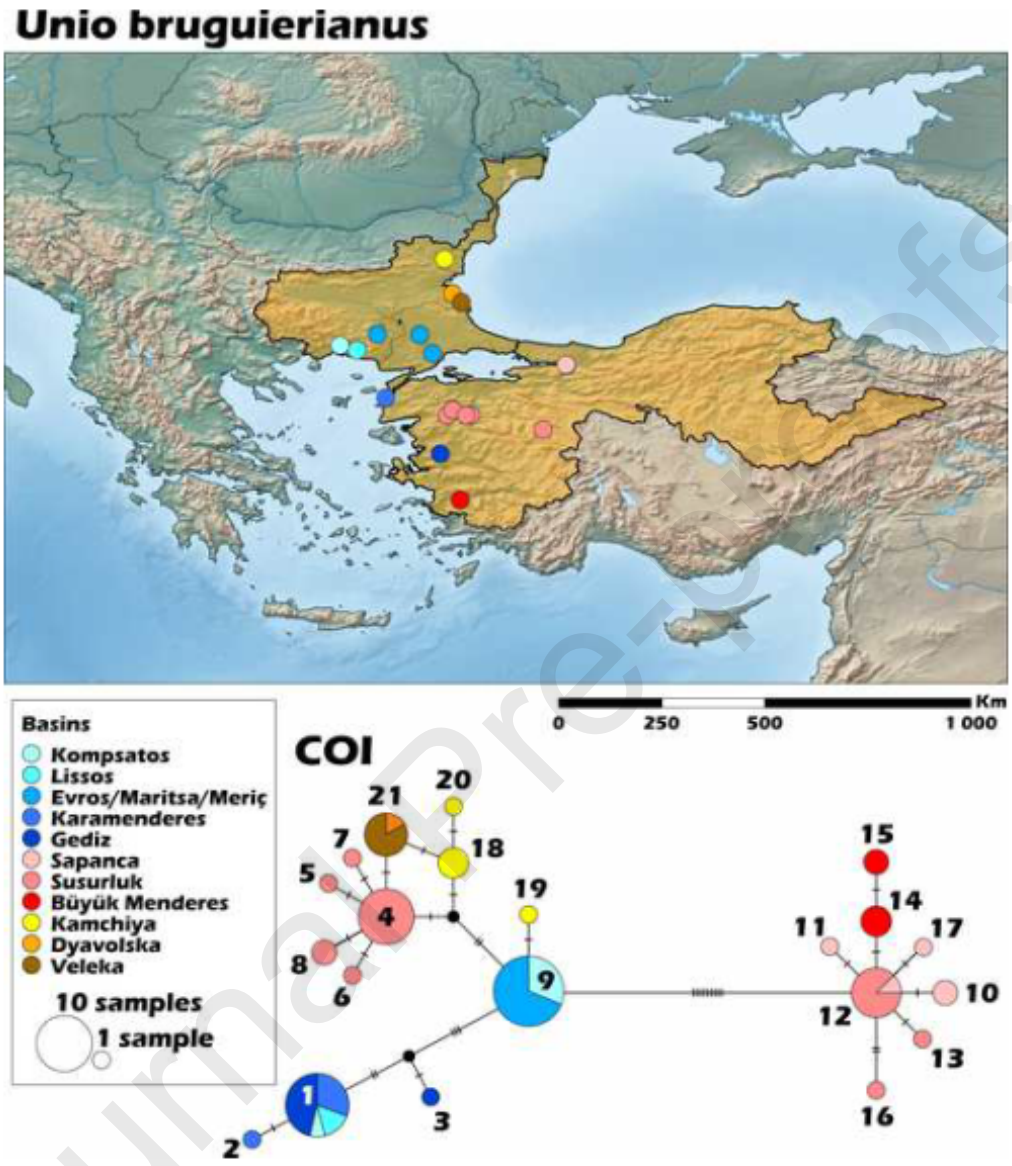

Figure 8

Click here to access/download;Figure;Figure 8. Hap Network + Map Carneus.jpg

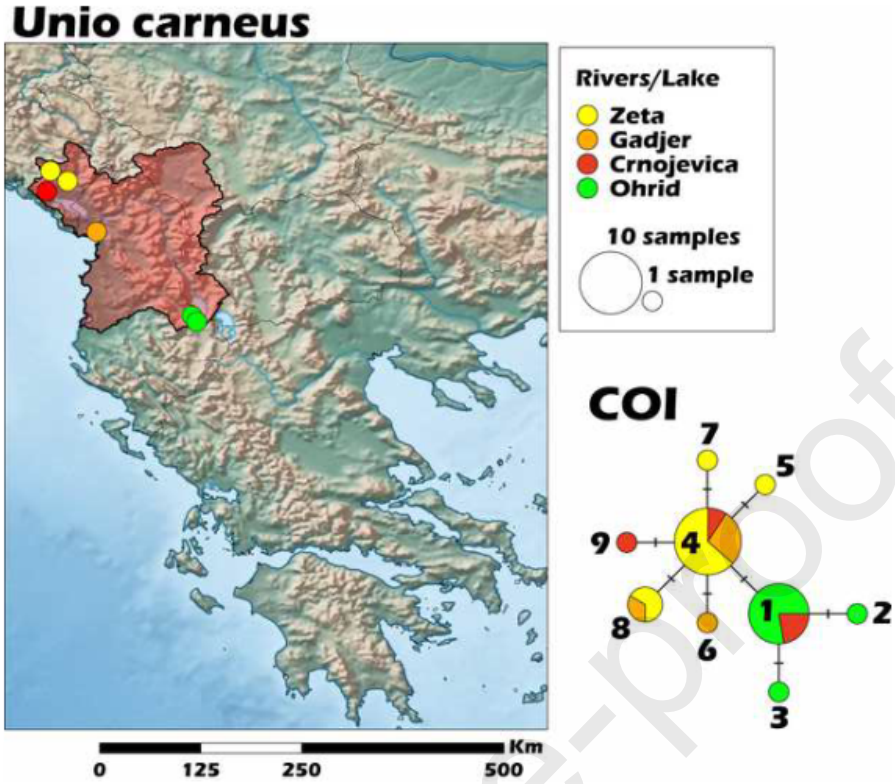

Figure 9

Click here to access/download;Figure;Figure 9. Hap Network + Map Crassus.jpg

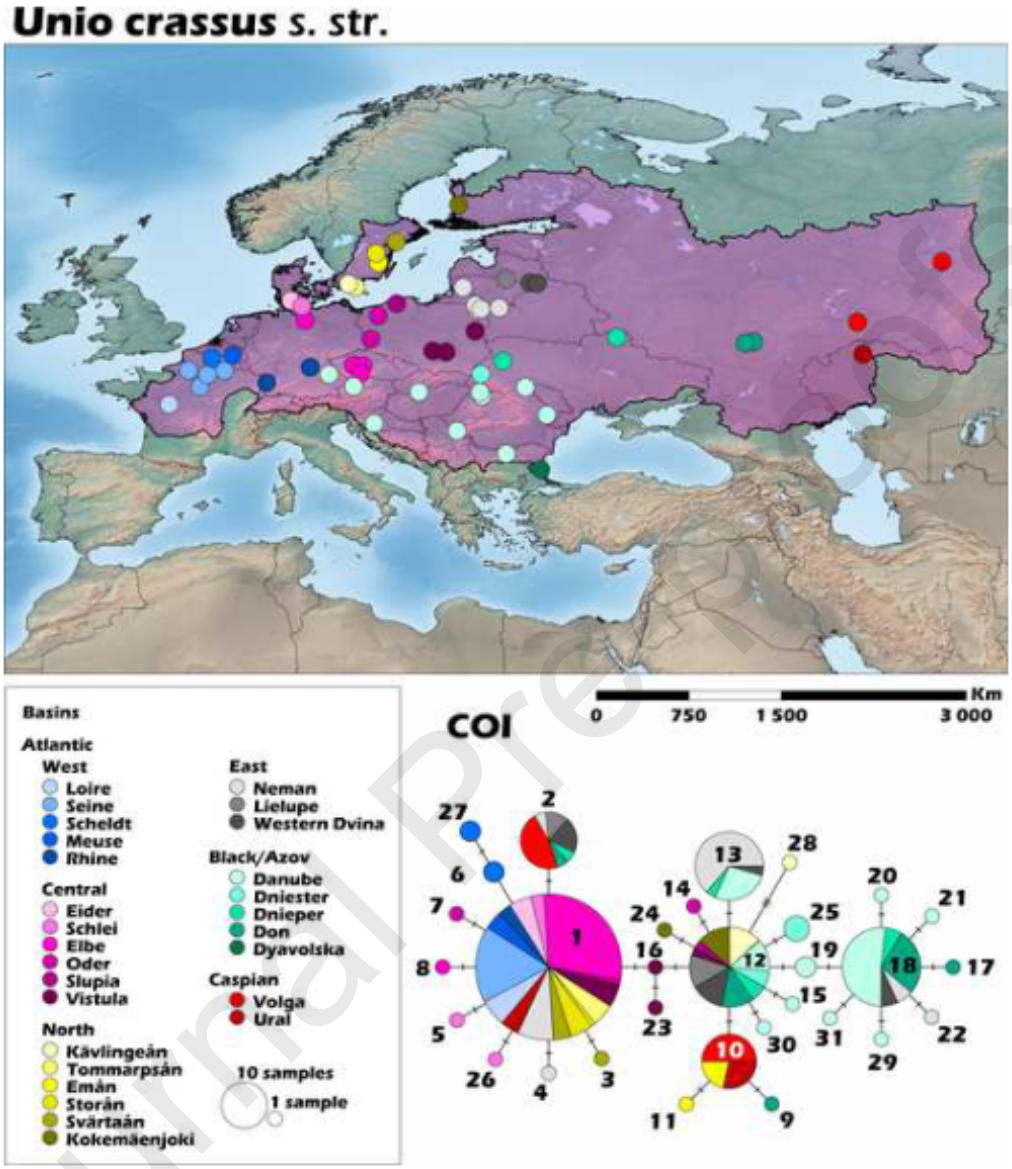

Figure 10

Click here to access/download;Figure;Figure 10. Hap Network + Map desectus.jpg

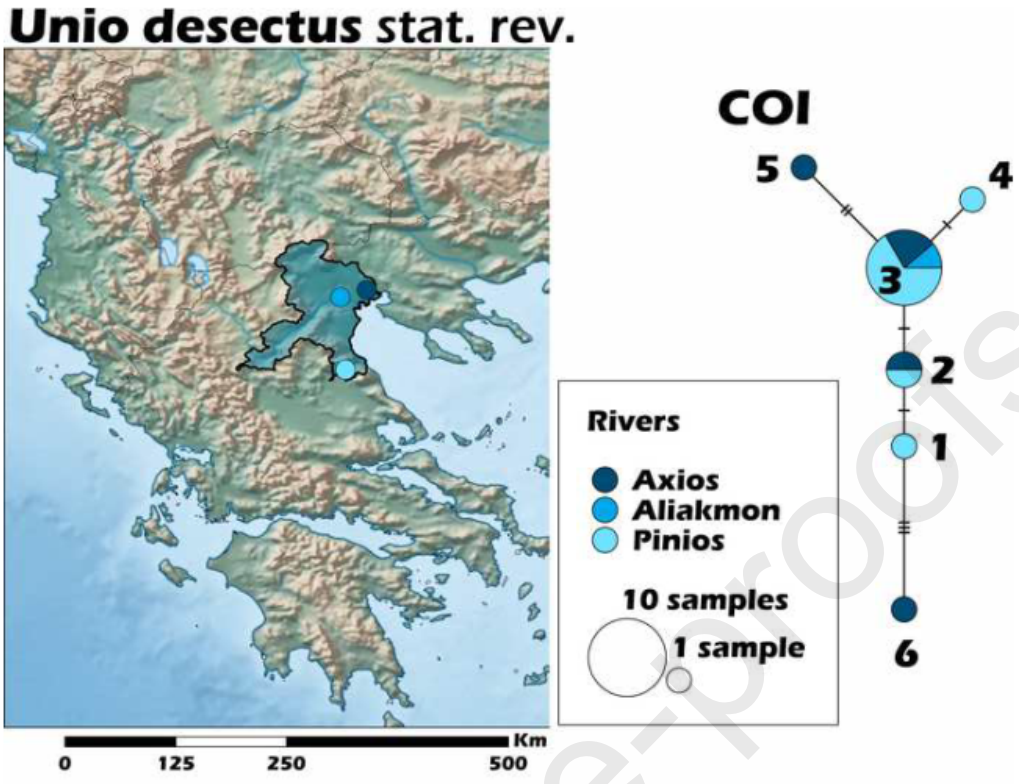

Figure 11

Click here to access/download;Figure;Figure 11. Hap Network + Map Gontierii.jpg

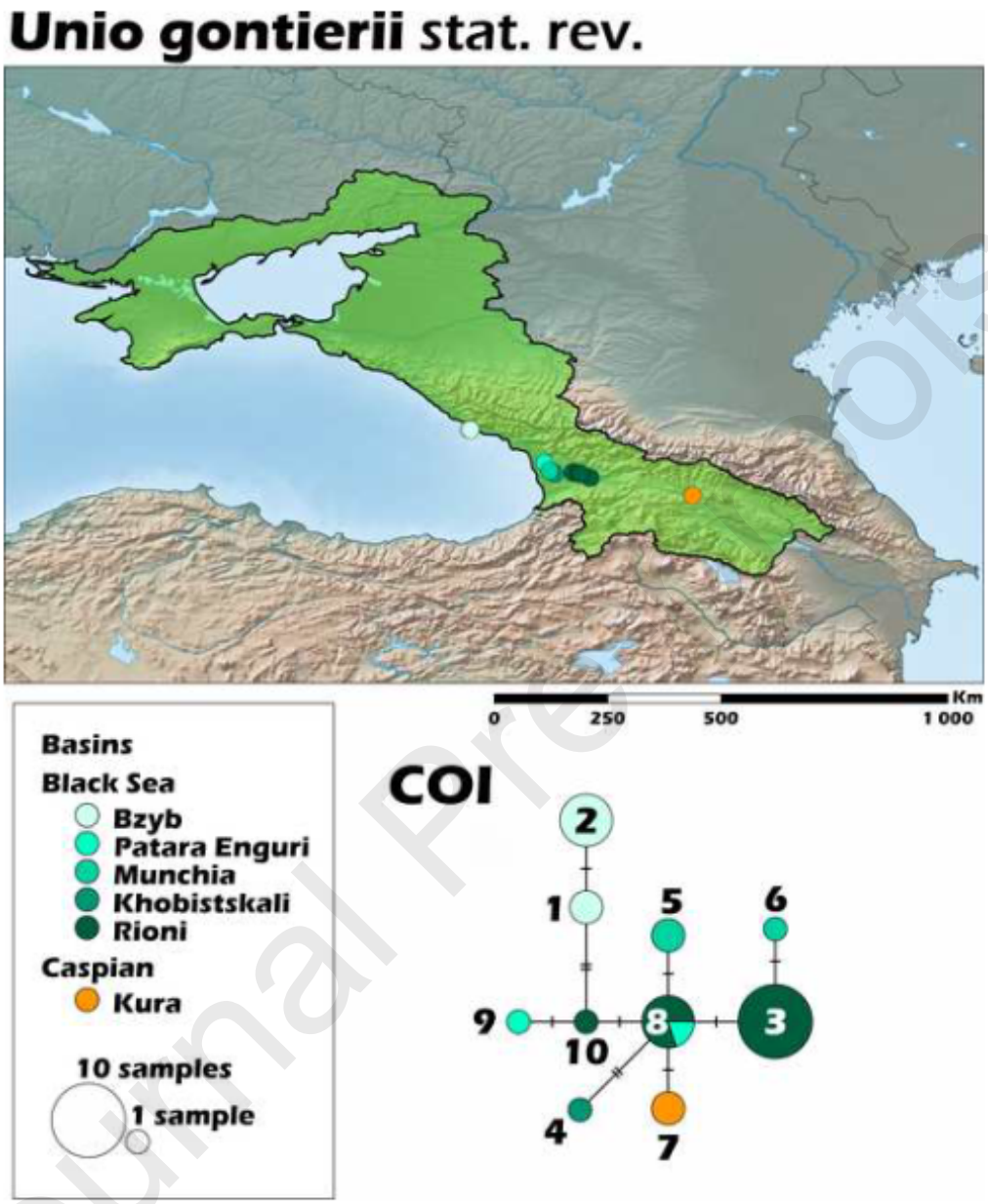

Figure 12

Click here to access/download;Figure;Figure 12. Hap Network + Map Ionicus.jpg

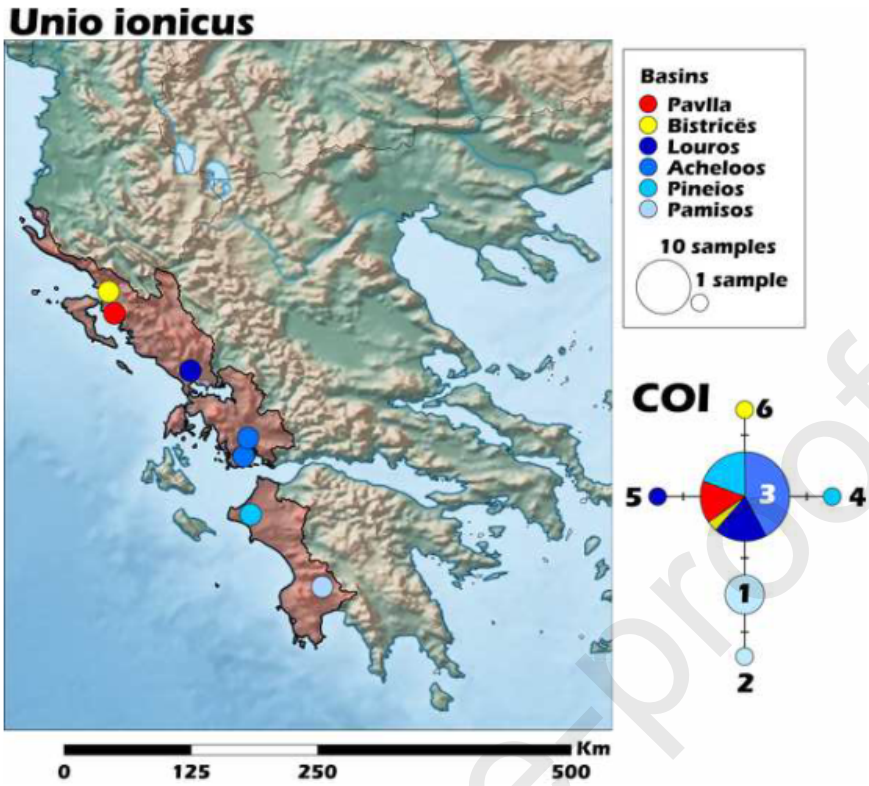

Figure 13

Click here to access/download;Figure;Figure 13. Hap Network + Map Mardinensis.jpg

Figure 14

Click here to access/download;Figure;Figure 14. Hap Network + Map Nanus.jpg

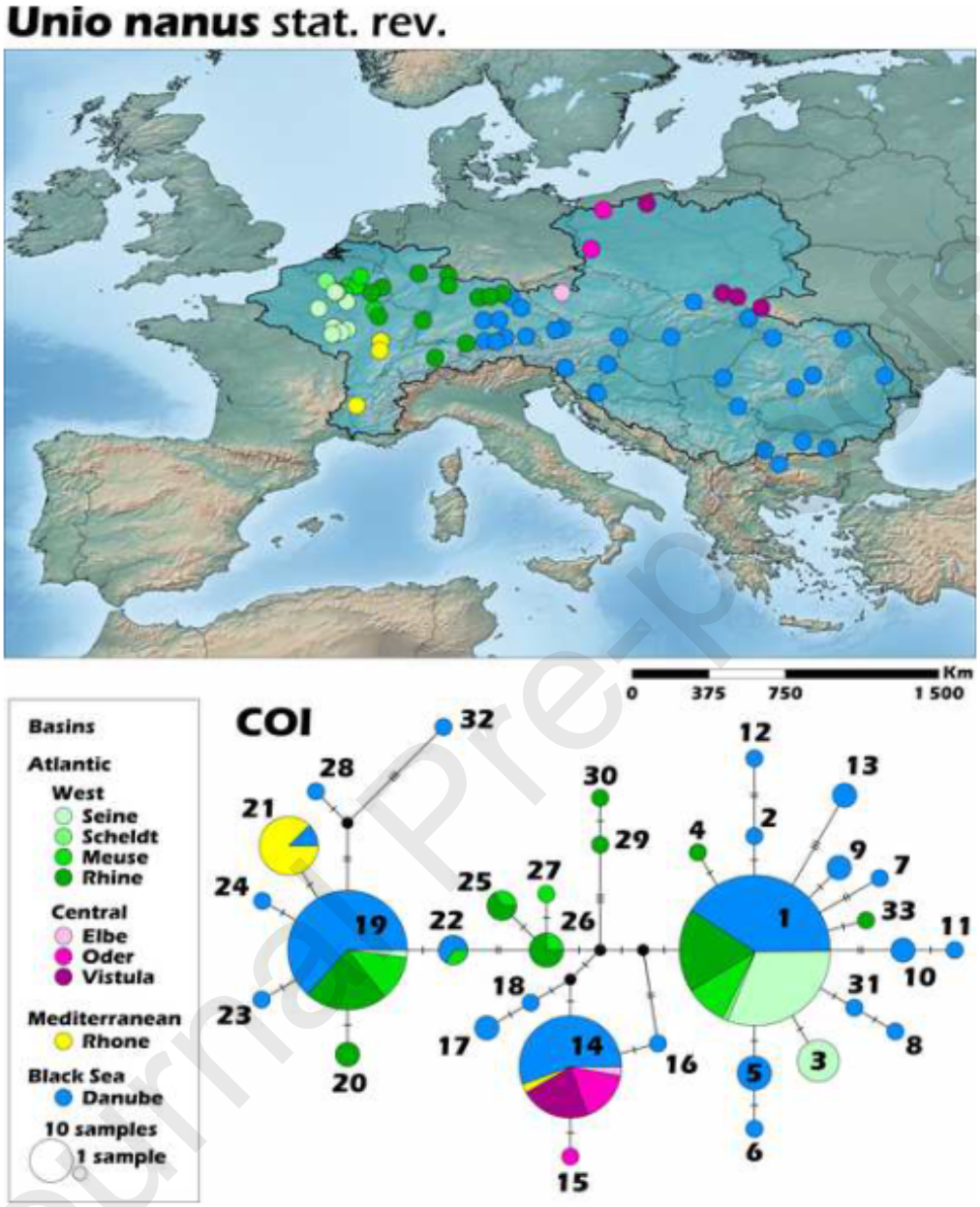

Figure 15

Click here to access/download;Figure;Figure 15. Hap Network + Map Tumidiformis.jpg

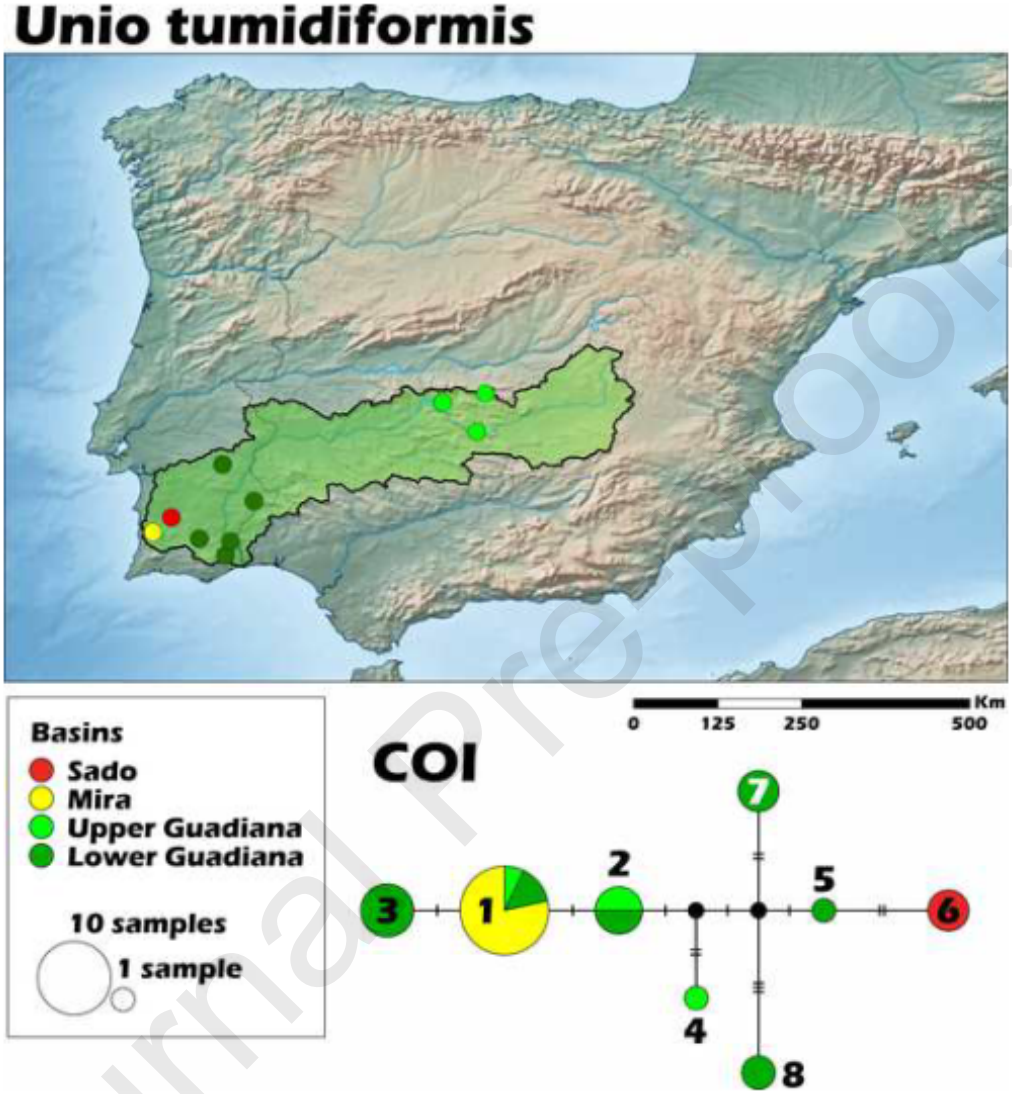

Figure 16

Click here to access/download;Figure;Figure 16. Hap Network + Map Vicarius.jpg

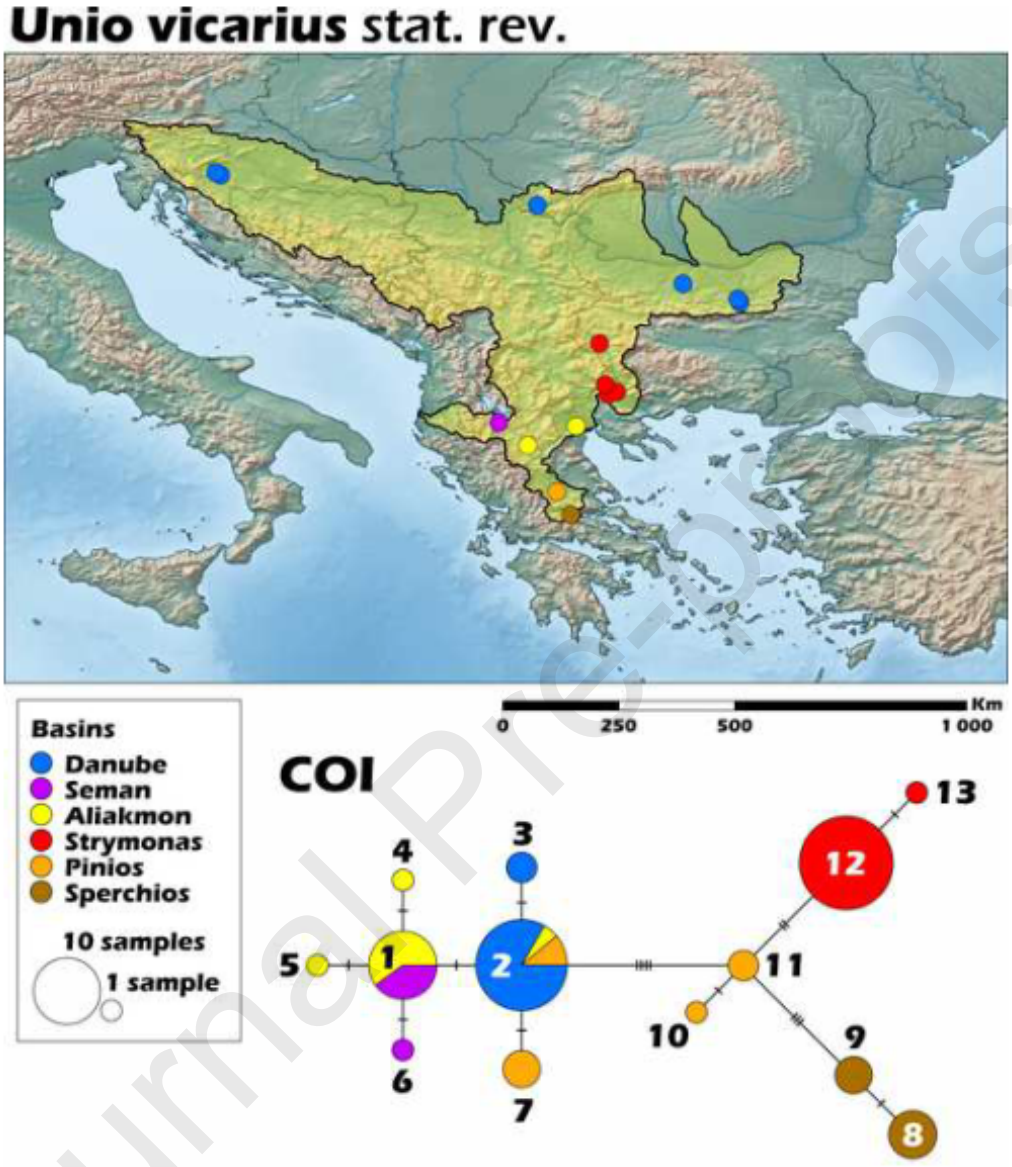

Graphical Abstract

Click here to access/download;Graphical Abstract;Graphical abstract.jpg